Quantitative proteome and PTMome analysis of *Arabidopsis thaliana* root responses to persistent osmotic and salinity stress.

Rodriguez, MC.[1*]., Mehta, D[1*]., Tan, M[1], and Uhrig, RG[1]

[#]Corresponding Authors:

*Denotes equal contribution

Dr. R. Glen Uhrig

Department of Biological Sciences
University of Alberta
Edmonton, Alberta
Canada
T6G 2E9

Phone: +1 780 492 3088
E-Mail: ruhrig@ualberta.ca

[1]Department of Biological Sciences, University of Alberta, Edmonton, Alberta, Canada

Running Title: Impact of Salt and Osmotic Stress on Root Proteome

ABSTRACT

Abiotic stresses such as drought result in large annual economic losses around the world. As sessile organisms, plants cannot escape the environmental stresses they encounter, but instead must adapt to survive. Studies investigating plant responses to osmotic and/or salt stress have largely focused on short-term systemic responses, leaving our understanding of intermediate to longer-term adaptation (24 h - days) lacking. In addition to protein abundance and phosphorylation changes, evidence suggests reversible lysine acetylation may also be important for abiotic stress responses. Therefore, to characterize the protein-level effects of osmotic and salt stress, we undertook a label-free proteomic analysis of *Arabidopsis thaliana* roots exposed to 300 mM Mannitol and 150 mM NaCl for 24 h. We assessed protein phosphorylation, lysine acetylation and changes in protein abundance, detecting significant changes in 245, 35 and 107 total proteins, respectively. Comparison with available transcriptome data indicates that transcriptome- and proteome-level changes occur in parallel, while PTMs do not. Further, we find significant changes in PTMs and protein abundance involve different proteins from the same networks, indicating a multifaceted regulatory approach to prolonged osmotic and salt stress. In particular, we find extensive protein-level changes involving sulphur metabolism under both osmotic and salt conditions as well as changes in protein kinases and transcription factors that may represent new targets for drought stress signaling. Collectively, we find that protein-level changes continue to occur in plant roots 24 h from the onset of osmotic and salt stress and that these changes differ across multiple proteome levels.

Key Words: ***Arabidopsis thaliana,*** **Protein Acetylation, Protein Phosphorylation, Post-Translational Modifications, Quantitative Proteomics**

INTRODUCTION

Environmental conditions contributing to abiotic stresses such as drought and salinity result in large annual economic losses around the world. Between 2005 and 2015, drought was responsible for 30 % of agricultural loss, totaling to USD 19.5 billion (Food and Agriculture Organization of the United Nations (FAO), 2017). The combined result of human activities and climate change represent two of the major environmental factors currently threatening global food security (Ghosh and Xu, 2014), with rising global temperatures extending drought periods and lengthening plant drought recovery time (Schwalm et al., 2017). More frequent and severe droughts have left farmers to depend on progressively unsustainable irrigation and fertilization practices to maintain crop yield, placing further stress on drainage patterns and salinity levels of farmland (Kaushal et al., 2018). Both drought and salinity stress create a hyperosmotic condition typically referred to as osmotic stress, while increased salinity has the additive effect of concurrently increasing ionic strength. These osmotic and ionic effects massively impede the ability of roots to take up water, forcing molecular, cellular and/or morphological changes in order to adapt and survive.

All plant organs must adapt to drought and salt stress; however, roots are at the forefront and are thus responsible for adjusting their molecular program as necessary to ensure whole plant survival. In particular, under water-limiting conditions, roots restructure their investment from lateral root formation to axile roots to forage deeper soil layers (Paez-Garcia et al., 2015). For example, overexpression of the cell wall expansion protein EXPA5 (AT3G29030), stimulates root cell elongation by lengthening the root tip rather than increasing cell number (Xu et al., 2014). While DEEPER ROOTING 1 (DRO1; AT1G72490), a rice quantitative trait locus, is capable of increasing root angle in response to gravity, creating a steeper and deeper root system architecture, in addition to a higher photosynthetic capability, less wilting, and a >30 % increase in filled grain under severe drought (Uga et al., 2013). Thus, root system changes help define the growth and structure of aboveground biomass.

Within all plant cells, proteins are at the heart of sensing and initiating signaling events that then launch stress-adaptive responses. While the majority of our understanding of system drought responses has been driven by transcriptomic responses (Kreps et al., 2002; Kilian et al 2007; Rest et al., 2016; Yin et al., 2019), integrating this knowledge with a protein-level understanding of a plant's environmental stress response and adaptation over time through quantitative proteomics, offers opportunities for both fundamental understanding and biotechnological application.

Osmotic and salt stress have a major influence over crop productivity worldwide (Ashraf and Akram, 2009), making it essential that we continue to refine our understanding of how plants respond to these perturbations in order to breed and/or engineer climate resilient crops. Emphasizing this need are the multiple studies that have examined the effects of osmotic and/or salt stress across a range of photosynthetic eukaryotes using both global and targeted analyses to understand the range of molecular, biochemical, physiological and morphological responses these stresses elicit (Zhang et al., 2012). This compendium of osmotic and salt stress data encompass a vast multitude of plant systems, time-frames and applied technologies, ranging from minutes to days of stress exposure (Jiang et al., 2007), followed by transcriptomic (Kilian et al., 2007; Kreps et al., 2002; Rest et al., 2016; Yin et al., 2019), proteomic (Jiang et al., 2007; Koh et al., 2015; Luo et al., 2015; Zhang et al., 2012) and metabolomic (Shelden et al., 2016) analyses to assess how the root environment responds to either abiotic stress. However, given the large variability in sampling time frames and root growth approaches, coupled with: 1) limited in-parallel examination of multiple stresses and proteoforms within the same study, 2) established disconnects

between temporal changes in transcripts and proteins (Baerenfaller et al., 2012; Petricka et al., 2012; Reiland et al., 2009; Seaton et al., 2018; Uhrig et al., 2019), and 3) limited investigations of the role post-translational modifications (PTMs) play in root osmotic and salt adaptation (Koh et al., 2015; Wu et al., 2016; Zhu, 2016), further quantitative proteomic analysis are required.

PTMs are a pillar of properly functioning eukaryotic cells. Of the known PTMs, protein phosphorylation and lysine acetylation are the two most abundant (Choudhary et al., 2009; Henriksen et al., 2012; Hartl et al., 2017; Sharma et al., 2014; Uhrig et al., 2019; Weinert et al., 2011), with plants maintaining a comparable phosphoprotein landscape to humans (PhosPhat, http://phosphat.uni-hohenheim.de/; (Heazlewood et al., 2008), ATHENA; http://athena.proteomics.wzw.tum.de/; (Mergner et al., 2020); Plant PTM Viewer, https://www.psb.ugent.be/webtools/ptm-viewer/; (Willems et al., 2019). More recently, global analysis of protein acetylation in Arabidopsis (Finkemeier et al., 2011; Hartl et al., 2017; Liu et al., 2018; Uhrig et al., 2019; Wu et al., 2011) and multiple crop species (Guo et al., 2020; Nallamilli et al., 2014; Singh et al., 2020; Smith-Hammond et al., 2014; Walley et al., 2018; Zhou et al., 2018; and Xue et al., 2018) have similarly identified thousands of lysine acetylation events occurring on proteins with diverse functions and subcellular localizations. These two highly abundant PTMs have also been found to intersect on proteins involved in the same cellular processes (Rao et al., 2014; Soufi et al., 2012; Tran et al., 2012; Uhrig et al., 2019) in addition to occurring on different proteins involved in the same metabolic pathways (Uhrig et al., 2019), suggesting protein phosphorylation and lysine acetylation are functionally intertwined on multiple scales.

To better understand osmotic and salt stress responses in roots, we endeavored to examine the intermediate-term responses (24 h) of *Arabidopsis thaliana* (Arabidopsis) roots subjected to either 300 mM Mannitol or 150 mM NaCl. Then using label-free quantitative (LFQ) proteomics, we quantified the changes in the Arabidopsis root proteome, phosphoproteome, and acetylome using an established sequential quantitative proteomic workflow to facilitate the simultaneous assessment of multiple proteoforms in the same study. Our findings demonstrate how protein abundance and PTMs change relative to one another and to the transcriptome, in addition to understanding intersections within, and between, each abiotic stress condition to reveal osmotic and/or salt-specific responses.

RESULTS

Quantification and localization of mannitol- and salt-induced protein phosphorylation, lysine acetylation and abundance changes

Twenty-one day old Arabidopsis seedlings grown in liquid MS media were subjected to either osmotic (300 mM mannitol)- or salt (150 mM NaCl)-stress for 24 h starting and ending at zeitgeber time 3 (ZT 3) and assessed for quantifiable changes in protein phosphorylation and/or lysine acetylation status as well as protein abundance (Figure 1A; Supplemental Table 1-3). We quantified a total of 3,681 phosphorylated peptides and 266 acetylated peptides across 1,291 and 201 proteins, respectively, with a PTM localization ≥ 0.75 (Supplemental Table 2-3), while a total of 3,128 proteins were quantified for changes in abundance (Supplemental Table 1). Of these, 3681 phospho- and 266 acetyl-peptides corresponding to 1291 and 201 proteins, respectively, exhibited significant changes under osmotic stress (*pval* ≤ 0.05; FC ≥ 1.5), while 3681 phosphorylated and 266 acetylated peptides found on 1291 and 201 proteins, respectively, exhibited significant change (*pval* ≤ 0.05; FC ≥ 1.5) under salt stress

(Figure 1B-D; Table 1; Supplemental Table 2-3). A total of 32 and 86 proteins exhibited significant changes in abundance (*pval* ≤ 0.05; FC ≥ 1.5) under osmotic and salt stress (Figure 1B-D; Table 1; Supplemental Table 1).

Next, we compared the Log_2 fold-change (log_2FC) distribution of significantly changing proteins and PTMs between osmotic- and salt-treated roots (Figure 1B-D). Analysis of proteins exhibiting a significant change in either abundance, phosphorylation or lysine acetylation found a total of 11 (11.5 %), 57 (30.3 %) and 11 (45.8 %) proteins overlapping between stress conditions (Figure 1B-D). Lastly, to understand where within the plant cell environment intermediate-term changes in the proteome are occurring, we obtained the predicted subcellular localization for all proteins exhibiting a significant change in PTM status or abundance under either osmotic- or salt-stress using SUBAcon (SUBA4; https://suba.live/; Hooper et al., 2014). Here, we found differences in the subcellular distribution of significantly changing proteins between each treatment (Figure 1E), with both mannitol and salt predominantly inducing changes in cytosolic, nuclear, and plasma membrane proteins. Salt also elicited changes in the greater numbers of plastidial and extracellular proteins, while mannitol had more changes in proteins localized to the vacuole (Figure 1E).

Overlap between changing PTMome and proteome is limited

Often, PTMs are quantified independent of assessing changes in proteome abundance. Therefore, reported changes in PTM levels may also be due to fluctuations in protein abundance. To better understand this here, we examined proteins exhibiting PTM changes for concurrent changes in protein abundance. Under osmotic stress 31 (21.9 %) and 17 (71 %) proteins exhibiting significant changes in either phosphorylation or lysine acetylation were also quantified at the proteome level to not be changing in abundance. No PTM modified proteins concurrently exhibited a significant change in PTM and protein abundance (Table 1). Similarly, under salt stress, 39 (24.4 %) and 13 (59 %) phosphorylated and acetylated proteins, respectively, were quantified in our proteome data to not be changing (Table 1). Our concurrent assessment of proteome and PTM abundance changes provides increased confidence that observed phosphorylation and lysine acetylation changes are related to PTM-level changes, and not changes in proteome abundance. Moreover, since assessing changes in PTMs requires enrichment of modified peptides, it is likely that the remainder of PTM modified proteins not observed in our protein abundance measurements are simply below detection.

Gene Ontology (GO) analysis of proteome and PTM fluctuations reveals differences between osmotic- and salt-induced stress.

To better understand what cell processes are changing at the proteome-level after 24 h of osmotic or salt stress, we performed a gene ontology (GO) enrichment analysis for biological process GO terms (Supplemental Table 4). In response to salt stress, we found a number of significantly enriched GO terms amongst proteins exhibiting a change in abundance. These include: response to osmotic stress (GO:0006970, sulfate reduction (GO:0019419), S-glycoside metabolic processes (GO:0016143), glucosinolate metabolic processes (GO:0019757), in addition to organonitrogen metabolism (GO:1901564), translation (GO:0006412), and translational elongation (GO:0006414) (Table 2). Similarly, under osmotic stress we see enrichment of organonitrogen compound catabolism (GO:1901565), sulfur compound metabolic processes (GO:0006790) and S-glycoside metabolic processes (GO:0016143) amongst the significantly changing proteins (Supplemental Table 4). At the

phosphoprotein level, salt stress induced changes in a number of biological processes. Here we saw significant enrichment of cyclic nucleotide metabolic processes (GO:0009187), protein phosphorylation (GO:0006468) and cell surface receptor signaling pathway (GO:0007166). Conversely, osmotic stress conditions saw the enrichment of cell division (GO:0051301), cell cycle (GO0007049) and cell cycle processes (GO:0022402). Next, we performed a protein domain analysis using Thalemine (https://bar.utoronto.ca/thalemine/). Here, we found an enrichment of a number of protein domains amongst the proteins significantly changing in abundance under salt stress (Supplemental Table 4). In particular, multiple chaperone and chaperonin domains as well as thioredoxin domains in addition to glycoside hydrolase superfamily, which supports our GO findings of augmented S-glycoside metabolic processes (GO:0016143) in salt stressed roots.

Comparative analysis of proteome and transcriptome changes reveals osmotic and salt-response disconnects.

It is well established that transcriptome and proteome changes are often disconnected in their temporal peak expression patterns (Baerenfaller et al., 2012; Graf et al., 2017; Seaton et al., 2018). Therefore, using publicly available microarray transcriptome data from Arabidopsis plants subjected to analogous stress treatments under similar growth conditions (Kilian et al., 2007), we performed a comparative analysis to better understand the temporal dynamics of the transcripts that correspond to proteins exhibiting phosphorylation, lysine acetylation or abundance changes upon 24 h of osmotic- or salt-stress. Despite being comparable, some differences exist between our experimental conditions and that of Kilian and colleagues (2007). These include: the use of a 12:12 photoperiod, 21 day old plants and stress application starting at zeitgeber (ZT) 3 in our study versus a 16:8 photoperiod, 18 day old plants and an unknown stress application start time by Kilian and colleagues (2007). Using this transcriptome data, we sought to cluster corresponding transcripts based on their expression dynamics and investigate how these dynamics were reflected at the level of protein abundance as well as lysine acetylation or phosphorylation status (Figure 2-3; Supplemental Table 5).

Under both osmotic- and salt-stress conditions, the majority of proteins exhibiting a significant change in abundance, phosphorylation and/or lysine acetylation 24 h post-stress maintained a minimal $\log_2$FC transcriptional change (Cluster 1 - Figure 2-3). We also saw protein clusters emerge under both osmotic- and salt-stress whereby an increasing trend in their transcript abundance from stress onset (0 h) to 24 h post-stress paralleled our observed end-point proteome abundance changes at 24 h (Cluster 2 - Figure 2-3). However, this was not case for protein phosphorylation and acetylation events, which did not parallel transcriptome changes in either the osmotic or salt stress treatments (Figure 2-3). By clustering the significantly changing proteome and PTMome based on their corresponding transcriptional expression profile from a comparably acquired, publicly available dataset, we find that transcript changes are generally a good indicator of proteome changes 24 h post-osmotic or -salt stress initiation in Arabidopsis roots. Conversely, we find that transcriptional changes are a poor indicator of PTM-level changes. Overall, our data finds that osmotic and salt-stress induced proteomes, when clustered by transcriptional change profile (0 h to 24 h), reveals key differences in how Arabidopsis roots respond to these stresses after 24 h.

Network analysis of proteins exhibiting osmotic- and salt-induced changes in PTM status and/or abundance reveals how the proteomes intersect

Next, using a combination of STRING-DB association network analyses (https://string-db.org/) and SUBA4 (https://suba.live/) protein subcellular localization information, we assembled subcellular localization-resolved protein association networks to elucidate the degree of interconnectedness between osmotic- and salt-induced PTM and protein abundance changes (Figure 4-5). Proteins with an edge score threshold of 0.5 or below were excluded from visualization. Here, we find that changes in the PTM status and/or protein abundance of metabolic proteins were most common between both osmotic and salt stress conditions (Figure 4-5). This is highlighted by proteins involved in both the transport and assimilation of sulfur as well as primary metabolism (Figure 4-5). Similarly, changes in transcription and protein translation were also common between osmotic and salt treatments. Lastly, we see a number of known drought responsive proteins to be changing in both our osmotic and salt condition, indicating that our treatment regimes elicited the expected responses.

Overall, our association networks further validate earlier GO enrichment analyses in addition to visualizing the strength of these relationships using compiled meta-association data between proteins. These networks also provided a means by which to integrate additional data types including: the type and degree of change in lysine acetylation, phosphorylation and/or abundance (outer ring), in addition to the subcellular localization of each protein within the plant cell (inner circle). Together, this data highlights the multi-dimensional relationships that exist between proteins exhibiting significant changes in either abundance or PTM status in response to osmotic and/or salt stress.

DISCUSSION

Benchmarking our data against known drought responsive proteins

The identification of the following proteins in our protein association networks suggests that our application of mannitol (300 mM) and salt (150 mM) was sufficient to elicit a stress response in 21 day old Arabidopsis plants. In our data, we find DROUGHT REPRESSED 4 (AtDR4; AT1G73330) a protease inhibitor protein that decreases in transcript abundance upon increasing drought (Frei dit Frey et al., 2010), to also decrease in protein abundance upon salt stress (Log_2FC = -1.02). PATATIN-RELATED PHOSPHOLIPASE A (pPLA; AT2G26560) which is involved in modulating Arabidopsis water status (Yang et al., 2012) is up-regulated under both osmotic (Log_2FC = 0.96) and salt (Log_2FC = 1.15) conditions (Supplemental Table 1). From a PTM perspective, SALT-OVERLY-SENSITIVE 1 (SOS1; AT2G01980), a plasma membrane Na(+)/H(+) antiporter (Shi et al., 2000) and characterized salt tolerance protein (Ullah et al ., 2016) that is activated by phosphorylation (Quintero et al 2011) increases in its phosphorylation status (Log_2FC = 2.7) after 24 h of salt treatment. Further, osmotic stress results in elevated SNF1-RELATED PROTEIN KINASE 2.2 (SNRK2.2; AT3G50500) phosphorylation (Log_2FC = 2.71). SNRK2.2 is a key activator of ABA signaling pathway that regulates responses such as stomatal closure (Kulik et al., 2011). We also see a decrease in the phosphorylation of TUDOR-SN PROTEIN 1 (TSN1; AT5G07350) under salt stress (Log_2FC = -0.96), which would suggest this is an activating PTM event, as TSN1 is known to regulate GIBBERELLIC ACID 20 OXIDASE 3 (GA20ox3; AT5G07200) expression under salt stress (Yan et al., 2014) (Supplemental Table 2). We further expand the role of TSN1 in this capacity beyond salt stress to also include osmotic stress, as we similarly see a decrease in phosphorylation (Log_2FC = -0.95). Lastly, PLASMA MEMBRANE INTRINSIC PROTEIN 2;7

(PIP2;7; AT4G35100), an aquaporin known to be involved in osmoregulation during drought and salinity stress and to be extensively modified by multiple PTMs (Di Pietro et al., 2013), exhibited a decrease in its lysine acetylation status under salt stress (Log_2FC = -3.28) (Supplemental Table 3). The fluctuation of these aforementioned proteins across the various proteomes we assessed provides confidence that our dataset contains novel protein-level insights into plant osmotic and salt stress responses. Further, the concerted changes in both the transcriptome and significantly changing proteome observed in both our osmotic or salt treatments, suggests our treatments are in line with previous osmotic and salt treatments, and demonstrates the utility of performing meta-analyses to more broadly understand and contextualize results.

Protein lysine acetylation is up-regulated on core facets of glycolysis under both osmotic and salt stress conditions

Protein lysine acetylation occurring on primary glycolytic enzymes is almost universally up-regulated under both osmotic and salt stress (Figure 1B). For example, under both osmotic and salt treatments, key metabolic enzymes between glyceraldehyde 3-phosphate and oxaloacetate, such as GLYCERALDEHYDE-3-PHOSPHATE DEHYDROGENASE C2 (GAPC2; AT1G13440; NaCl_Log_2FC = 1.19), PHOSPHOGLYCERATE KINASE 3 (PGK3; AT1G79550; MAN_Log_2FC = -0.69), ENOLASE 2 (LOS2; AT2G36530; MAN_Log_2FC = 0.74, NaCl_Log_2FC = 2.95), and PHOSPHOENOLPYRUVATE CARBOXYLASE (PPC1; AT1G53310; NaCl_Log_2FC = 1.60) all have upregulated lysine acetylation events. Similarly, UDP-GLUCOSE PYROPHOSPHORYLASE 1 (UGP1; AT3G03250; MAN_Log_2FC = 3.02, NaCl_Log_2FC =3.56) also shows an unidirectional up-regulation in acetylation status under both applied stresses (Figure 4-5; Supplemental Table 3).

Protein lysine acetylation has recently become established as a regulatory PTM in plants and other organisms (Finkemeier et al., 2011, Hartl et al., 2017; Zhao et al., 2010). Catalyzed by acetyltransferases, protein acetylation requires the primary metabolite acetyl-CoA. Acetyl CoA is a central intermediate metabolite between catabolic and anabolic pathways and as such, it is uniquely placed to exert either feedback or feedforward regulation through reversible protein acetylation. Interestingly, we see two key metabolic enzymes directly connected to acetyl-CoA metabolism to exhibit decreases in their acetylation status under osmotic or salt stress (Figure 4 and 5). These include: CITRATE SYNTHASE 3 (CSY3; AT2G42790; MAN_Log_2FC = -2.06) and ATP-CITRATE LYASE B-1 (ACLB-1; AT3g06650; NaCl_Log_2FC = -0.94). Multiple studies have found that protein N^{ε} acetylation is an abundant PTM across plants (De Boor et al., 2015; Finkemeier et al., 2011; Hartl et al., 2017; Li et al., 2018; Uhrig et al., 2019; Wu et al., 2011). In particular, glycolytic and specialized metabolic proteins have been found to be extensively acetylated under nitrogen stress in tea leaves (Jiang et al., 2018) as well as in a diel manner across a number of facets of plant metabolism in *Arabidopsis thaliana*, including N^{ε} acetylation of GAPC in roots (Uhrig et al., 2019). Here, our data suggest that N^{ε} acetylation also plays a role in salt and osmotic stress response in plants through primary metabolism. Interestingly, N^{α} protein acetylation has also been connected to drought resistance and is suggested to be ABA stress responsive (Linster et al., 2015; Linster et al., 2020). Since both N^{α} and N^{ε} protein acetylation rely on acetyl-CoA as an acetate donor, there likely exists higher-level intersections between these two forms of protein acetylation. Highlighting this possibility is the recent discovery of dual-specificity GNAT acetyltransferases in Arabidopsis (Bienvenut et al., 2020).

Sulfur metabolism needed for short- and intermediate-term drought response

During drought stress, ABA is synthesized in the roots and then transported to the shoots to induce stomatal closure (Agurla et al., 2018). However, ABA biosynthesis in the roots requires sulfur. Plant root sulfate assimilation is primarily driven by ADENOSINE 5'PHOSPHOSULFATE REDUCTASE (APR), which reduces sulfate to sulfite followed by further reduction to sulfide by FERREDOXIN DEPENDENT SULFITE REDUCTASE (SiR) (Takahashi et al., 2011). Sulfide is then fixed by O-acetylserine(thiol)lyase into Cysteine (Cys) (Chan et al., 2013) to act as the sulfur donor for the sulfuration of molybdenum cofactor (Moco) sulfurase (Xiong et al., 2001), which is then necessary to initiate ABSCISIC ALDEHYDE OXIDASE 3 (AAO3) (Mendel, 2002; Schwarz and Mendel, 2006) and the ultimate production of ABA.

Studies have determined that Cys levels attune ABA biosynthesis (Batool et al., 2018; Cao et al., 2014), which in turn, limits sulfur assimilation at the level of APR (Takahashi et al., 2011). APR enzymatic activity is driven by the demand for sulfur, meaning that the uptake and assimilation of sulfur during drought is likely foundational to the short-term drought response. At 24 h of NaCl stress, we observed a number of key sulfur assimilating enzymes to decrease in their protein abundance, including: ATP SULFURYLASE 1 (APS1; AT3G22890; Log_2FC = -1.43), APR1 (AT4G04610; Log_2FC = -1.56), APR2 (AT1G62180; Log_2FC = -1.39) and APR3 (AT4G21990; Log_2FC = -1.80) and ADENOSINE 5'-PHOSPHOSULFATE KINASE (APK; AT2G14750 Log_2FC = -1.60) (Figure 4-5; Supplemental Table 1). Furthermore, SULFATE TRANSPORTER 1;2 (SULTR1;2; AT1G78000), which mediates the uptake of the environmental sulfate by plant roots, is reduced in abundance (Log_2FC = -0.90) under salt stress. Osmotic stress also induced sulfur related enzyme changes. SULTR1;1 exhibited an increase in protein abundance (Log_2FC = 1.56), while APR1 was reduced in abundance similar to that observed under salt stress (Log_2FC = -1.15). This suggests that by 24 h post salt-stress initiation plants have already transitioned from utilizing short-term adaptations, to implementing longer term solutions.

Transcriptionally, APR is regulated by sulfur availability (Hirai et al., 2003), demand for Cys (Davidian and Kopriva, 2010), and also in response to environmental stressors such as high salt (Koprivova et al., 2008). Specifically, Koprivova and colleagues (2008) reported a 3-fold increase in APR mRNA after 5 h of 150 mM NaCl in Arabidopsis roots. Using the AtGenExpress Arabidopsis stress expression dataset (Kilian et al 2007), we calculated a peak expression of APR transcripts at 6 h post 150 mM NaCl stress initiation, which then was found to continually decrease through to 24 h (Kilian et al., 2007; Supplemental Table 5). Interestingly, an opposing trend in shoot APR expression is observed (Kilian et al., 2007). While APR in roots peaks soon after high salt exposure, APR in shoots remains low until eventually peaking at 24 h. This points to APR and sulfur driven drought-responses acting as a short-term responder in the roots and an intermediate responder in the shoots. Given this, a sharp increase in root APR levels may facilitate the sulfur assimilation required for ABA production, which then leads to prompt stomatal closure. A later peak in shoot APR may be useful for intermediate drought response mechanisms, such as reducing reactive oxygen species (ROS).

Salt stress is also known to increase the production of oxidative enzymes (e.g. NADPH oxidase), which are necessary for signaling and response during abiotic stress (Mittova et al., 2003), with subsequent reduction in ROS required as the salt stress persists (Hasegawa and Bressan, 2000). To mitigate the damaging effects of ROS, plants can produce glutathione (GSH), an antioxidant derived from Glu, Cys, and Gly. Stress-induced GSH production requires sulfur-containing Cys, with high levels of Cys found to enhance synthesis of GSH in plants (Takahashi et

al., 2011). Demand for both, Cys and GSH, reciprocally regulates sulfur assimilation through APR (Davidian and Kopriva, 2010), with depletion of GSH pools under prolonged drought stress conditions driving the production of APR (Chan et al., 2013). Thus, upregulation of APR activity in the shoots may contribute to the production of antioxidants such as GSH. Further time-course experimentation is required to fully elucidate the interplay between salt-induced sulfur metabolism changes at the protein level in roots versus shoots, and is beyond the scope of this study.

Both osmotic and salt stresses induce high-levels of UDP-glucose pyrophosphorylase (UGP1) lysine acetylation

We find that UGP1 (AT3G03250) maintained some of the largest increases in lysine acetylation, with salt (Log_2FC = 3.58) and osmotic (Log_2FC = 3.03) stress both eliciting large changes to UGP1 acetylation (Figure 2-3). UGP1 activity has previously been found to be regulated by PTMs. For example, phosphorylation by Per-Arnt-Sim (PAS) kinase downregulates UGP1 activity resulting in a net decrease of glycogen in yeast (Rutter et al., 2002). Analysis of available osmotic- and salt-stress induced transcript data found limited changes in UGP1 transcript levels under mannitol (-0.35) and salt (-0.15) treatments 24 h post stress initiation (Kilian et al., 2007); however, UGP1 transcripts are also known to be a poor indicator of protein-level or enzyme activity changes (Ciereszko et al., 2001).

UGP1 is an ubiquitous enzyme found in plants, animals, and bacteria that produces UDP-glucose (Meng et al., 2009), which is the direct substrate for trehalose synthesis (Schluepmann and Matthew, 2009). Thus, activation of UGP1 may be linked to increased trehalose biosynthesis in osmotic- and salt-stressed roots. In *E. coli,* trehalose stabilizes proteins and prevents protein aggregation during osmotic stress (Moruno Algara et al., 2019). This is also true for resurrection plants such as *Myrothamnus flabellifolius* where trehalose functions as a protectant to stabilize membranes and proteins, allowing them to survive during dehydration-rehydration cycles (Figueroa and Lunn, 2016; O'Hara et al., 2013). There is evidence that trehalose synthesis in Arabidopsis may serve a similar function during drought stress (Lin et al., 2019). Furthermore, knockdown of UGP1 in *S. cerevisiae* results in a reduction in trehalose as well as a reduction in oxidative stress resistance (Yi and Huh, 2015), suggesting that UGP1 involvement in mitigating osmotic stress is an evolutionary conserved mechanism.

In plants, stachyose and raffinose family oligosaccharides (RFO) are degraded by UGP1 (PWY-6527; https://biocyc.org/), releasing diphosphate. Thus an upregulation of UGP1 protein-levels and/or adjustments to its activity could serve as a homeostatic mechanism for adjusting the nutritional status of a plant under drought stress. Alternatively, if UGP1 lysine acetylation decreases functionality, it may increase RFO content in the cell. RFOs are suggested to have a dual role as osmoprotectants and compatible solutes (Elsayed et al., 2014). Other groups have found higher RFO content in desiccated plant tissues (Obendorf and Gorecki, 2012) and that RFOs stabilize membranes during dehydration (Pluskota et al., 2015). Overall, our data suggests that UGP1 functionality may be regulated by reversible lysine acetylation under both osmotic and salt stress conditions. However, whether UGP1 lysine acetylation increases or decreases UGP1 activity, and how that activity confers osmotic protection, is beyond the scope of this study.

Lysine acetylation of GTP-Proteins may support root tip mitotic division

In Arabidopsis, GTP hydrolysis by Ran and Ran binding protein complexes are important in the regulation of auxin-induced mitotic progression in root tips (Kim and Roux, 2003; Xu et al., 2016). GTP hydrolysis by Ran facilitates protein import and release into the nucleus (Clarke and Zhang, 2008). Moreover, Ran facilitates mitotic spindle assembly by promoting the release of spindle assembly factors from importin complexes in the nucleus (Carazo-Salas et al., 1999). The role of Ran in mitotic spindle assembly has been proposed as an important role in root growth during drought stress (Akashi et al., 2016), and to intersect with ABA response and drought tolerance (Luo et al., 2013). In particular, both AtRAN1 and AtRAN3 are known to be induced by salt treatment, with *ran1/ran3* double mutants showing higher sensitivity to salt treatment, displaying significantly reduced root growth after being treated for 5 days with 100 mM NaCl (Xu et al., 2016).

Our data supports the involvement of RAN-GTPases in osmotic and salt stress responses. In particular, we find SIRANBP (AT1G07140) and RAN3 (AT5G55190) to be acetylated under salt (Log_2FC = 1.92 SIRANBP; Log_2FC = 3.68 AtRAN3) and mannitol (Log_2FC = 1.81 SIRANBP; Log_2FC = 3.65 RAN3) treatment (Figure 4-5). Phylogenetic analysis of RAN-GTPases Rab domains finds a 81 % (≤ 3 residue change) sequence homology between unicellular eukaryotes to vertebrates (Coppola et al., 2018), rendering it interesting that Ran GTPases in humans and mice are also regulated by reversible protein acetylation (De Boor et al., 2015). Human Ran possesses 5 lysine (K) acetylation sites: K37, K60, K71, K99, and K159 (Choudhary et al., 2009; PHOSIDA, http://www.phosida.com). Each site provides a different regulatory mechanism, for example, AcK159 increases HsRan binding towards Importin-β enhancing substrate import and release into the nucleus (De Boor et al. 2015). A global alignment between HsRan1 and AtRAN3 shows 81.6 % sequence similarity with HsK159 and AtK162 sharing an equivalent position (EMBL-EBI, Needle; Madeira et al., 2019). At the present moment, there are no studies reporting the effects of AcK162 on AtRAN3 in relation to osmotic or salt stress, however, considering the high sequence similarity between HsRan1 and AtRAN3 it is likely that AtRAN is regulated by lysine acetylation, and that this AcK162 may be responsible for increased mitotic division driven by RAN GTPase activity. Therefore, our observation of increased AtRAN-GTPase lysine acetylation may be a mechanism by which plants drive root elongation under drought stress conditions.

ABF3 phosphorylation may aid in the intermediate and long term drought response

As a last resort, plants can launch the drought-escape (DE) response when tolerance or avoidance becomes an improbable solution to drought stress (Kooyers, 2015). DE is an adaptive mechanism that shifts the program from vegetative growth to reproductive growth triggering early flowering (Shavrukov et al., 2017). By shortening their life cycle they can set seed before the stress leads to their inevitable death. In rice, ABA promotes DE through positive regulation of flowering genes (Du et al., 2018). In Arabidopsis, the molecular mechanisms of DE are yet to be fully understood, nonetheless it is clear that under drought conditions Arabidopsis can favor early flowering (Kenney et al., 2014; Verslues and Juenger, 2011). Riboni et al. (2016) found ABA is capable of activating DE response by promoting transcriptional up-regulation of GIGANTEA (GI; AT1G22770) and florigen genes such as FLOWERING LOCUS T (FT; AT1G65480) and TWIN SISTER OF FT (TSF; AT4G20370) (Ribonu et al., 2016). A separate early flowering pathway involves ABA signaling through the expression and activity of ABSCISIC ACID RESPONSIVE ELEMENT-BINDING FACTOR 3/4 (ABF3; AT4G34000, ABF4; AT3G19290) transcription factors

(Hwang et al., 2019). ABF3/4 interacts with the NF-Y complex to bind to the promoter of SUPPRESSOR OF CONSTANS 1 (SOC1; AT2G45660) and initiate early flowering. In our data, we find ABF3 phosphorylated as a result of salt and osmotic stress (NaCl_Log_2FC = 3.89, MAN_Log_2FC = 2.95). It is possible that ABF3 phosphorylation may promote the initiation of early flowering pathways needed for DE response. ABA induced multifaceted regulatory networks, such as florigen genes or direct activation of SOC1 transcription, may be necessary to ensure early flowering under drought-stress conditions.

Alternatively, up-regulation of ABF3 phosphorylation may be needed for drought avoidance (DA). ABFs also target the ABA- responsive regulatory *cis*- element (ABRE) and coordinate drought stress and ABA responses (Fernando et al., 2018; Liu et al., 2018). For instance, ABF3 directly regulates the expression of proteins, such as AtTPP1 (AT5G10100), which is required for the adjustment of stomatal aperture and primary root architecture (Lin et al., 2020, Kerr et al., 2018). ABA-dependent phosphorylation sites have been previously identified, with some sites conferring specificity to individual upstream kinases. For example, SNF1-RELATED KINASE 2 (SnRK2; AT3G50500) phosphorylates multiple conserved RXXS/T sites on ABF3 during ABA-dependent response to drought stress (Furihata et al. 2006; Uno et al. 2000; Yoshida et al., 2015). OPEN STOMATA 1 (OST1; AT4G33950) kinase phosphorylates ABF3 on multiple LXRXXpS/T preferred motifs including T451 (Sirichandra et al., 2010). As such, ABF3 controls part of the ABA-regulated transcriptome as an OST1 substrate. Calcium-dependent protein kinases 6 (CPK6; AT2G17290) also phosphorylates a subset of ABA-signaling related transcription factors, including ABF3 (Zhang et al., 2020). CPK6 phosphorylates ABF3 on preferred LXRXXpS/T motifs with the following sites identified: S32, S126, S134, and T169. However, we see ABF3 phosphorylated on S332, S338, and T342 (Supplemental Table 2), suggesting that these phosphorylation sites may be drought specific and the responsible protein kinases are unknown.

In the context of the 24 h stress presented in this study, it is more likely that an up-regulation of ABF3 phosphorylation is part of the plants DA response. Since ABF3 can be phosphorylated by multiple kinases, such as OST1 (Chen et al., 2013), CPK6 (Zhang et al., 2020), and SnKR2 (Fujii et al., 2009), it is probable that different phosphorylation events occur under DE and DA. The classification of DE and DA as discrete drought tolerance responses is unrealistic since a plant can employ a combination of DE and DA at different stages of its life cycle (Shavrukov et al., 2017). Thus it is probable that ABF3 phosphorylation is needed for both. Further research beyond the scope of this study is needed to identify the specific effect of these ABF3 phosphorylation events and the pathways that are initiated under DE and DA.

Diverse PTM catalyzing enzymes exhibit abundance or phosphorylation status fluctuations in response to osmotic and salt stress.

Our dataset uncovered a number of PTM modifying enzymes such as protein kinases (PKs; AT4G06744, AT5G48540, AT1G33590), phosphatases (AT3G45190) and ubiquitin ligases (AT2G23140) to change in overall abundance in response to either osmotic and/or salt stress. In particular, leucine rich-repeat (LRR) family protein AT4G06744, which decreases in abundance under both osmotic (Log_2FC = -1.25) and salt stress (Log_2FC = -3.73) and is exclusively root expressed (Klepikova Arabidopsis Atlas eFP browser - bar.utoronto.ca; Supplemental Table 1), but is otherwise uncharacterized. We also observe a decrease in the abundance of root development regulator

PLANT U-BOX 4 (PUB4) an E3 ubiquitin ligase under salt treatment (Log_2FC = -0.77), that when absent results in enhanced root growth (Kinoshita et al., 2015), suggesting that by 24 h, deregulation of root elongation has already been initiated at the protein level. Interestingly, the same authors suggest that PUB4 may intersect with auxin signaling to regulate root elongation, which would coincide with the extensive phosphorylation increases we observed on auxin related protein PILS2 (At1g71090; MAN_Log_2FC = 4.21), TOM1-LIKE 4 (AT1G76970; MAN_Log_2FC = 3.34, NaCl_Log_2FC = 3.47) and AT1G79020 (MAN_Log_2FC = 3.48, NaCl_Log_2FC = 3.61) (Figure 5-6; Supplemental Table 2).

Our analysis of the osmotic and salt induced phosphoproteomes also revealed a number of protein kinases that possess osmotic and/or salt induced changes in their phosphorylation status, which aligns with our enrichment related biological processes (Supplemental Table 4). In particular, we observed 12 PKs and 1 ubiquitin ligase (AT1G22500) to change in their phosphorylation status under osmotic stress, while 17 PKs and 1 ubiquitin ligase (AT1G22500) changed in their phosphorylation status under salt stress, of which, only 5 are common between both stresses, indicating either stress has wide ranging impacts on a number of PKs and that there are distinct differences in the PKs impacted by each stress. With the majority of these PKs representing plasma membrane localized protein kinases that are uncharacterized it is likely that these represent key initiators of the phospho-signaling cascades that help determine ubiquitous and specialized responses to osmotic and/or salt stress. In particular, CANNOT RESPOND TO DMBQ 1 (CARD1 / HPCA1; AT5G49760; MAN_Log_2FC = 3.54, NaCl_Log_2FC = 2.45), which is phosphorylated under both osmotic and salt stress conditions and was recently resolved as a hydrogen peroxide sensor kinase (Wu et al., 2020), making it logical that the increase in phosphorylation is likely related to its activation under these stress regimes. This also renders the other uncharacterized PKs potentially exciting targets for further characterization.

Lastly, a number of previously characterized PKs were also resolved in our dataset as specific to either mannitol or salt treatment. Under mannitol treatment this includes: CALCIUM DEPENDENT PROTEIN KINASE 3 (CPK3; AT4G23650; Log_2FC = 0.95), CAMODULIN-DOMAIN PROTEIN KINASE 9 (CPK9; AT3G20410; Log_2FC = -0.75) and MAP3K EPSILON PROTEIN KINASE (MAP3KE1; AT3G13530; Log_2FC = -1.14) (Figure 5; Supplemental Table 2) and CDK-ACTIVATING KINASE 4 (CAK4; AT1G66750; Log_2FC = 1.25) under salt stress conditions (Figure 6; Supplemental Table 2). With increased H_2O_2 leading to increased intracellular Ca^{2+} (Wu et al., 2020), it is likely that CPK3 and CPK9, both exhibiting high levels of root expression (Klepikova Arabidopsis Atlas eFP browser - bar.utoronto.ca), represent important intermediaries in converting Ca^{2+} signaling responses to cellular outcomes. In particular, CPK3, which has been implicated in ABA promoted stomatal closure (Mori et al., 2006) and CPK9 which has a negative role in ABA-mediated stomatal closure (Chen et al., 2019). Our phosphoproteome data extend these opposing roles for CPK3 and 9 to root osmotic stress response through their opposing changes in phosphorylation status under osmotic stress (Figure 6; Supplemental Table 2). Lastly, we observe increased phosphorylation of CAK4 under salt stress. Given the central role of CAK4 in regulating cell division, and its expression in the root apical meristem, our data suggests that its phosphorylation likely promotes its cell division activity in order to drive root elongation under salt stress (Takatsuka et al 2009, Sofroni et al., 2020).

Overall, it is clear that protein phosphorylation and a subselection of protein kinases are particularly important in osmotic and salt stress response 24 h after initiation. Unlike PKs that may have exhibited transcriptional

up-regulation, the subselection of PKs we observe here as changing in their abundance or phosphorylation status, represent excellent new candidates for future targeted characterization studies.

CONCLUSION

Here, we describe proteomic and PTMomic changes occurring in Arabidopsis roots exposed to 300 mM mannitol and 150 mM NaCl for 24 h. By examining intermediate proteome responses, we have uncovered a number of intriguing candidate proteins and PTM events for future investigations, in addition to resolving new extended function for proteins with known roles in either osmotic or salt stress responses, and by extension, ABA signaling. that may be key to longer-term survival under osmotic and/or salt stress conditions. Furthermore, we show lysine acetylation to be a potentially interesting PTM in osmotic- or salt-stress response, with stress-induced changes having been particularly focused on key primary metabolic enzymes. In undertaking this quantitative analysis of the proteome, phosphoproteome and acetylome, we were able to capture a wide swath of the intermediate term protein responses in a single study. Moving forward, understanding the intermediate to long-term responses of either osmotic and/or salt stress at the protein-level through time-course experimentation, is especially important for the development of new climate resilient crops.

MATERIALS & METHODS

Plant Growth and Harvesting

Arabidopsis thaliana Col-0 seeds were imbibed 2 days at 4 ^{o}C in the dark prior to growth in Magenta boxes containing 0.5 x MS media containing 0.5 % (w/v) sucrose. Plants were grown at 22 ^{o}C under a 12 h light : 12 h dark photoperiod for 21 days prior to the application of 0.5 x MS media containing 300 mM mannitol (osmotic) or 150 mM NaCl (salt). Seedlings were grown in either experimental or control media for an additional 24 h, with stresses beginning and ending at zeitgeber time 3 (ZT 3). Roots were manually separated from shoots and immediately frozen in liquid N_2. Roots were then ground in a mortar and pestle under liquid N_2 and stored at -80 ^{o}C until further use.

Sample Preparation and PTM Affinity Enrichments

Root tissue (800 mg) was extracted, processed and digested with trypsin (Promega) as previously described (Uhrig et al., 2019). Subsequent enrichment of phosphorylated or acetylated peptides was performed using titanium dioxide (NP-Ti02; Sachtopore; SNX 030S 005 #9205/1639) and anti-acetylated lysine IgG-coupled agarose (ICP0388; ImmuneChem, https://www.immunechem.com) as previously described (Uhrig et al., 2019), prior to analysis by mass spectrometry.

Liquid Chromatography MS/MS

A total of 1 µg of re-suspended peptide was injected by an Easy-nLC 1000 system (Thermo Scientific) and separated on a Thermo Scientific™ EASY-Spray™ HPLC Column (75 µm x 500 mm; particle size 2.0 µm; E803A). The column was equilibrated with 100 % solvent A (0.1 % formic acid (FA) in water). Peptides were eluted using the following gradient of solvent B (0.1 % FA in ACN): 0-50 min; 0-25 % B, 50-60 min; 25-32 % B, 60-70 min; 32-98 % B at a flow rate of 0.3 µl/min. High accuracy mass spectra were acquired with an Orbitrap Fusion (Thermo

Scientific) that was operated in data dependent acquisition mode. All precursor signals were recorded in the Orbitrap using quadrupole transmission in the mass range of 300-1500 m/z. Spectra were recorded with a resolution of 120 000 at 190 m/z, a target value of 4E5 and the maximum cycle time was set to 3 seconds. Data dependent MS/MS were recorded in the linear ion trap using quadrupole isolation with a window of 2 Da and HCD fragmentation with 30 % fragmentation energy. The ion trap was operated in rapid scan mode with a target value of 3E4 and a maximum injection time of 100 ms. Precursor signals were selected for fragmentation with a charge state from +2 to +7 and a signal intensity of at least 1E4. A dynamic exclusion list was used for 30 seconds and maximum parallelizing ion injections was activated.

Mass Spectrometry Data Analysis

Raw data were processed using MaxQuant software version 1.6.14.0 (http://www.maxquant.org/; Cox and Mann, 2008) and searched against The Arabidopsis Information Resource (TAIR10) protein database concatenated with a decoy database supplemented with contaminants using the Andromeda search engine. Fixed modifications included carbamidomethylation of cysteine residues, while methionine oxidation (all searches), lysine acetylation (acetylated peptide enrichments) and phosphorylated serine / threonine and tyrosine (phosphopeptide enrichments) were set as variable modifications, respectively. One missed cleavage for phosphoproteomic and proteomic measurements and two missed cleavages for lysine-acetylated peptides were permitted. A protein and PSM false discovery rates (FDR) threshold of 1 % was used, while match between runs and re-quantify options were enabled. Further downstream analysis was performed using Perseus version 1.6.14.0 (Tyanova et al., 2016). This involved the removal of reverse hits and contaminants, followed by $\log_2$-transformation, assembly into treatment groups and filtering based on the presence of measured data in at least 2 replicates of at least one group. Data were then median normalized, followed by imputation of missing values based on the normal distribution function set to default parameters. All PTM analyses utilized a PTM site localization score threshold ≥ 0.75. Significant changes in either protein or PTM peptide levels between each treatment condition and the control samples were assessed by Student's T-test (*pval* ≤ 0.05). Mass spectrometry data acquired for this study can be found at the EMBL proteomic repository Proteomics IDEntifications (PRIDE; https://www.ebi.ac.uk/pride/archive/; PXD019139).

Bioinformatics

To identify the biological functions of proteins changing in abundance, phosphorylation or lysine acetylation, a gene ontology (GO) analysis of biological processes was performed using the ONTOLOGIZER (http://ontologizer.de; (Bauer et al., 2008). A parent–child intersection analysis approach was used (Benjamini–Hochberg *FDR* correction *pval* ≤ 0.05). Clustering of Arabidopsis microarray time-course data was performed using a trajectory-based longitudinal clustering algorithm implemented in the kml-shape package in R (Genolini et al., 2016). For inputs, microarray counts were obtained from (Kilian et al., 2007) and fold changes were calculated for each time point comparing treated samples versus the controls. The resulting dataset was filtered based on the set of proteins that were found to significantly change in either abundance, phosphorylation or lysine acetylation status at 24 h. The resulting transcript fold-changes over the time-course were used to create four clusters based on the transcript trajectories over the 1, 3, 6, 12 and 24 h time points previously obtained (Kilian et al., 2007). Clustered trajectories and corresponding protein data were plotted using the *ggplot2* and *cowplot* packages in R version 3.3.1 (R Core

Team 2016). Further characterization of connections between quantified and significantly changing phospho- and acetyl-proteins was performed through association network analyses using the Cytoscape StringDB plugin StringApp (http://apps.cytoscape.org/apps/stringapp; Szklarczyk et al., 2017) with an overallStringDB association score threshold of 0.8. Cytoscape 3.8.2 (http://www.cytoscape.org/) visualized networks were then supplemented with subcellular localization data obtained from SUBAcon (http://suba.live/; (Hooper et al., 2014)

ACKNOWLEDGEMENT

The authors would like to thank the Functional Genomics Center Zurich for helpful discussions and the National Science and Engineering Research Council of Canada (NSERC) for funding this research.

CONFLICTS OF INTEREST

The authors declare they have no conflicts of interest

LITERATURE CITED

Agurla, S., Gahir, S., Munemasa, S., Murata, Y., and Raghavendra, A.S. (2018) Mechanism of Stomatal Closure in Plants Exposed to Drought and Cold Stress BT - Survival Strategies in Extreme Cold and Desiccation: Adaptation Mechanisms and Their Applications.

Akashi, K., Yoshimura, K., Kajikawa, M., Hanada, K., Kosaka, R., Kato, A., et al. (2016) Potential involvement of drought-induced Ran GTPase CLRan1 in root growth enhancement in a xerophyte wild watermelon. *Biosci Biotechnol Biochem*. 80: 1907–1916.

Ashraf, M., and Akram, N.A. (2009) Improving salinity tolerance of plants through conventional breeding and genetic engineering: An analytical comparison. *Biotechnol Adv*. 27: 744–752.

Baerenfaller, K., Massonnet, C., Walsh, S., Baginsky, S., Bühlmann, P., Hennig, L., et al. (2012) Systems-based analysis of Arabidopsis leaf growth reveals adaptation to water deficit. *Mol Syst Biol*. 8.

Bao, X., Liu, H., Liu, X., Ruan, K., Zhang, Y., Zhang, Z., et al. (2018) Mitosis-specific acetylation tunes Ran effector binding for chromosome segregation. *J Mol Cell Biol*. 10: 18–32.

Batool, S., Uslu, V.V., Rajab, H., Ahmad, N., Waadt, R., Geiger, D., et al. (2018) Sulfate is incorporated into cysteine to trigger ABA Production and stomatal closure. *Plant Cell*. 30: 2973–2987.

Bauer, S., Grossmann, S., Vingron, M., and Robinson, P.N. (2008) Ontologizer 2.0 - A multifunctional tool for GO term enrichment analysis and data exploration. *Bioinformatics*. 24: 1650–1651.

Bienvenut, W. V, Brünje, A., Boyer, J., Mühlenbeck, J.S., Bernal, G., Lassowskat, I., et al. (2020) Dual lysine and N-terminal acetyltransferases reveal the complexity underpinning protein acetylation. *Mol Syst Biol*. 16: 1–23.

Cao, M.J., Wang, Z., Zhao, Q., Mao, J.L., Speiser, A., Wirtz, M., et al. (2014) Sulfate availability affects ABA levels and germination response to ABA and salt stress in Arabidopsis thaliana. *Plant J*. 77: 604–615.

Carazo-Salas, R.E., Guarguaglini, G., Gruss, O.J., Segref, A., Karsenti, E., and Mattaj, L.W. (1999) Generation of GTP-bound ran by RCC1 is required for chromatin-induced mitotic spindle formation. *Nature*. 400: 178–181.

Chan, K.X., Wirtz, M., Phua, S.Y., Estavillo, G.M., and Pogson, B.J. (2013) Balancing metabolites in drought : the sulfur assimilation conundrum. *Trends Plant Sci*. 18: 18–29.

Chen, D.H., Liu, H.P., and Li, C.L. (2019) Calcium-dependent protein kinase CPK9 negatively functions in stomatal abscisic acid signaling by regulating ion channel activity in Arabidopsis. *Plant Mol Biol*. 99: 113–122.

Chen, Y.T., Liu, H., Stone, S., and Callis, J. (2013) ABA and the ubiquitin E3 ligase KEEP on GOING affect proteolysis of the Arabidopsis thaliana transcription factors ABF1 and ABF3. *Plant J*. 75: 965–976.

Choudhary, C., Kumar, C., Gnad, F., Nielsen, M.L., Rehman, M., Walther, T.C., et al. (2009) Lysine

acetylation targets protein complexes and co-regulates major cellular functions. *Science (80-)*. 325: 834–840.

Ciereszko, I., Johansson, H., Hurry, V., and Kleczkowski, L.A. (2001) Phosphate status affects the gene expression, protein content and enzymatic activity of UDP-glucose pyrophosphorylase in wild-type and pho mutants of Arabidopsis. *Planta*. 212: 598–605.

Clarke, P.R., and Zhang, C. (2008) Spatial and temporal coordination of mitosis by Ran GTPase. *Nat Rev Mol Cell Biol*. 9: 464–477.

Coppola, U., Caccavale, F., Scelzo, M., Holland, N.D., Ristoratore, F., and D'Aniello, S. (2018) Ran GTPase, an eukaryotic gene novelty, is involved in amphioxus mitosis. *PLoS One*. 13: 1–13.

Cox, J., and Mann, M. (2008) MaxQuant enables high peptide identification rates, individualized p.p.b.-range mass accuracies and proteome-wide protein quantification. *Nat Biotechnol*. 26: 1367–1372.

Davidian, J.C., and Kopriva, S. (2010) Regulation of sulfate uptake and assimilation - The same or not the same? *Mol Plant*. 3: 314–325.

De Boor, S., Knyphausen, P., Kuhlmann, N., Wroblowski, S., Brenig, J., Scislowski, L., et al. (2015) Small GTP-binding protein Ran is regulated by posttranslational lysine acetylation. *Proc Natl Acad Sci U S A*. 112: E3679–E3688.[1]

Di Pietro, M., Vialaret, J., Hem, S., Prado, K., Rossignol, M., Maurel, C., et al. (2013) Coordinated post-translational responses of aquaporins to abiotic and nutritional stimuli in arabidopsis roots. *Mol Cell Proteomics*. 12: 3886–3897.

Du, H., Huang, F., Wu, N., Li, X., Hu, H., and Xiong, L. (2018) Integrative Regulation of Drought Escape through ABA-Dependent and -Independent Pathways in Rice. *Mol Plant*. 11: 584–597.

Elsayed, A.I., Rafudeen, M.S., and Golldack, D. (2014) Physiological aspects of raffinose family oligosaccharides in plants: Protection against abiotic stress. *Plant Biol*. 16: 1–8.

Fernando, V.C.D., Al Khateeb, W., Belmonte, M.F., and Schroeder, D.F. (2018) Role of Arabidopsis ABF1/3/4 during det1 germination in salt and osmotic stress conditions. *Plant Mol Biol*. 97: 149–163.

Figueroa, C.M., and Lunn, J.E. (2016) A tale of two sugars: Trehalose 6-phosphate and sucrose. *Plant Physiol*. 172: 7–27.

Finkemeier, I., Laxa, M., Miguet, L., Howden, A.J.M., and Sweetlove, L.J. (2011) Proteins of diverse function and subcellular location are lysine acetylated in Arabidopsis. *Plant Physiol*. 155: 1779–1790.

Food and Agriculture Organization of the United Nations (FAO) (2017) The Impact of disasters and crises on agriculture and Food Security.

Frei dit Frey, N.F., Muller, P., Jammes, F., Kizis, D., Leung, J., Perrot-Rechenmann, C., et al. (2010) The RNA binding protein tudor-Sn is essential for stress tolerance and stabilizes levels of stress-responsive mRNAs encoding secreted proteins in Arabidopsis. *Plant Cell*. 22: 1575–1591.

Fujii, H., Chinnusamy, V., Rodrigues, A., Rubio, S., Antoni, R., Park, S.Y., et al. (2009) In vitro reconstitution of an abscisic acid signalling pathway. *Nature*. 462: 660–664.

Furihata, T., Maruyama, K., Fujita, Y., Umezawa, T., Yoshida, R., Shinozaki, K., et al. (2006) Abscisic acid-dependent multisite phosphorylation regulates the activity of a transcription activator AREB1. *Proc Natl Acad Sci U S A*. 103: 1988–1993.

Gebert, M., Dresselhaus, T., and Sprunck, S. (2008) F-actin organization and pollen tube tip growth in Arabidopsis are dependent on the gametophyte-specific armadillo repeat protein ARO1. *Plant Cell*. 20: 2798–2814.

Genolini, C., Ecochard, R., Benghezal, M., Driss, T., Andrieu, S., and Subtil, F. (2016) kmlShape: An efficient method to cluster longitudinal data (Time-Series) according to their shapes. *PLoS One*. 11: 1–24.

Ghosh, D., and Xu, J. (2014) Abiotic stress responses in plant roots: A proteomics perspective. *Front Plant Sci*. 5: 1–13.

Gnad, F., Gunawardena, J., and Mann, M. (2011) PHOSIDA 2011: The posttranslational modification database. *Nucleic Acids Res*. 39: 253–260.

Gorecka, K.M., Konopka-Postupolska, D., Hennig, J., Buchet, R., and Pikula, S. (2005) Peroxidase activity

of annexin 1 from Arabidopsis thaliana. *Biochem Biophys Res Commun*. 336: 868–875.
Graf, A., Coman, D., Uhrig, R.G., Walsh, S., Flis, A., Stitt, M., et al. (2017) Parallel analysis of *Arabidopsis* circadian clock mutants reveals different scales of transcriptome and proteome regulation. *Open Biol*. 7: 160333.
Guo, W., Han, L., Li, X., Wang, H., Mu, P., Lin, Q., et al. (2020) Proteome and lysine acetylome analysis reveals insights into the molecular mechanism of seed germination in wheat. *Sci Rep*. 10: 1–15.
Hartl, M., Füßl, M., Boersema, P.J., Jost, J., Kramer, K., Bakirbas, A., et al. (2017) Lysine acetylome profiling uncovers novel histone deacetylase substrate proteins in Arabidopsis . *Mol Syst Biol*. 13: 949.
Hasegawa, P.M., and Bressan, R.A. (2000) Plant Cellular and Molecular Responses to High Salinity. *Annu Rev Plant Biol*. 51: 463–499.
Heazlewood, J.I., Durek, P., Hummel, J., Selbig, J., Weckwerth, W., Walther, D., et al. (2008) PhosPhAt : A database of phosphorylation sites in Arabidopsis thaliana and a plant-specific phosphorylation site predictor. *Nucleic Acids Res*. 36: 1015–1021.
Henriksen, P., Wagner, S.A., Weinert, B.T., Sharma, S., Bačinskaja, G., Rehman, M., et al. (2012) Proteome-wide analysis of lysine acetylation suggests its broad regulatory scope in saccharomyces cerevisiae. *Mol Cell Proteomics*. 11: 1510–1522.
Hirai, M.Y., Fujiwara, T., Awazuhara, M., Kimura, T., Noji, M., and Saito, K. (2003) Global expression profiling of sulfur-starved Arabidopsis by DNA macroarray reveals the role of O-acetyl-L-serine as a general regulator of gene expression in response to sulfur nutrition. *Plant J*. 33: 651–663.
Hooper, C.M., Tanz, S.K., Castleden, I.R., Vacher, M.A., Small, I.D., and Millar, A.H. (2014) SUBAcon: A consensus algorithm for unifying the subcellular localization data of the Arabidopsis proteome. *Bioinformatics*. 30: 3356–3364.
Hwang, K., Susila, H., Nasim, Z., Jung, J.Y., and Ahn, J.H. (2019) Arabidopsis ABF3 and ABF4 Transcription Factors Act with the NF-YC Complex to Regulate SOC1 Expression and Mediate Drought-Accelerated Flowering. *Mol Plant*. 12: 489–505.
Jiang, J., Gai, Z., Wang, Y., Fan, K., Sun, L., Wang, H., et al. (2018) Comprehensive proteome analyses of lysine acetylation in tea leaves by sensing nitrogen nutrition. *BMC Genomics*. 19: 1–13.
Jiang, Y., Yang, B., Harris, N.S., and Deyholos, M.K. (2007) Comparative proteomic analysis of NaCl stress-responsive proteins in Arabidopsis roots. *J Exp Bot*. 58: 3591–3607.
Kaushal, S.S., Likens, G.E., Pace, M.L., Utz, R.M., Haq, S., Gorman, J., et al. (2018) Freshwater salinization syndrome on a continental scale. *Proc Natl Acad Sci U S A*. 115: E574–E583.
Kenney, A.M., Mckay, J.K., Richards, J.H., and Juenger, T.E. (2014) Direct and indirect selection on flowering time, water-use efficiency (WUE, δ13C), and WUE plasticity to drought in Arabidopsis thaliana. *Ecol Evol*. 4: 4505–4521.
Kerr, T.C.C., Abdel-Mageed, H., Aleman, L., Lee, J., Payton, P., Cryer, D., et al. (2018) Ectopic expression of two AREB/ABF orthologs increases drought tolerance in cotton (Gossypium hirsutum). *Plant Cell Environ*. 41: 898–907.
Kilian, J., Whitehead, D., Horak, J., Wanke, D., Weinl, S., Batistic, O., et al. (2007) The AtGenExpress global stress expression data set: Protocols, evaluation and model data analysis of UV-B light, drought and cold stress responses. *Plant J*. 50: 347–363.
Kim, D., Ntui, V.O., Zhang, N., and Xiong, L. (2015) Arabidopsis Yak1 protein (AtYak1) is a dual specificity protein kinase. *FEBS Lett*. 589: 3321–3327.
Kim, S.H., and Roux, S.J. (2003) An Arabidopsis Ran-binding protein, AtRanBP1c, is a co-activator of Ran GTPase-activating protein and requires the C-terminus for its cytoplasmic localization. *Planta*. 216: 1047–1052.
Kinoshita, A., Ten Hove, C.A., Tabata, R., Yamada, M., Shimizu, N., Ishida, T., et al. (2015) A plant u-box protein, pub4, regulates asymmetric cell division and cell proliferation in the root meristem. *Dev*. 142: 444–453.
Koh, J., Chen, G., Yoo, M.J., Zhu, N., Dufresne, D., Erickson, J.E., et al. (2015) Comparative Proteomic Analysis of Brassica napus in Response to Drought Stress. *J Proteome Res*. 14: 3068–3081.
Konopka-Postupolska, D., Clark, G., Goch, G., Debski, J., Floras, K., Cantero, A., et al. (2009) The role of

annexin 1 in drought stress in Arabidopsis. *Plant Physiol*. 150: 1394–1410.
Kooyers, N.J. (2015) The evolution of drought escape and avoidance in natural herbaceous populations. *Plant Sci*. 234: 155–162.
Koprivova, A., North, K.A., and Kopriva, S. (2008) Complex signaling network in regulation of adenosine 5′-phosphosulfate reductase by salt stress in arabidopsis roots. *Plant Physiol*. 146: 1408–1420.
Kreps, J.A., Wu, Y., Chang, H.S., Zhu, T., Wang, X., and Harper, J.F. (2002) Transcriptome changes for Arabidopsis in response to salt, osmotic, and cold stress. *Plant Physiol*. 130: 2129–2141.
Kulik, A., Wawer, I., Krzywińska, E., Bucholc, M., and Dobrowolska, G. (2011) SnRK2 protein Kinases - Key regulators of plant response to abiotic stresses. *Omi A J Integr Biol*. 15: 859–872.
Lee, S., Lee, E.J., Yang, E.J., Lee, J.E., Park, A.R., Song, W.H., et al. (2004) Proteomic of identification of annexins, calcium-dependent membrane binding proteins that mediate osmotic stress and abscisic acid signal transduction in arabidopsis. *Plant Cell*. 16: 1378–1391.
Li, X., Ye, J., Ma, H., and Lu, P. (2018) Proteomic analysis of lysine acetylation provides strong evidence for involvement of acetylated proteins in plant meiosis and tapetum function. 142–154.
Lin, Q., Wang, S., Dao, Y., Wang, J., and Wang, K. (2020) Arabidopsis thaliana trehalose-6-phosphate phosphatase gene TPPI enhances drought tolerance by regulating stomatal apertures. *J Exp Bot*. 71: 4285–4297.
Lin, Q., Yang, J., Wang, Q., Zhu, H., Chen, Z., Dao, Y., et al. (2019) Overexpression of the trehalose-6-phosphate phosphatase family gene AtTPPF improves the drought tolerance of Arabidopsis thaliana. *BMC Plant Biol*. 19: 1–15.
Linster, E., Layer, D., Bienvenut, W. V., Dinh, T. V., Weyer, F. A., Wiebke, L., et al. (2020) The Arabisopsis N-acetyltransferase NAA60 locates to the plasma membrane and is vital for the high salt stress response. *New Phytol*. 2: 554-546.
Linster, E., Stephan, I., Bienvenut, W. V., Maple-Grødem, J., Myklebust, L.M., Huber, M., et al. (2015) Downregulation of N-terminal acetylation triggers ABA-mediated drought responses in Arabidopsis. *Nat Commun*. 6.
Liu, S., Lv, Z., Liu, Y., Li, L., and Zhang, L. (2018) Network analysis of ABA-dependent and ABA-independent drought responsive genes in Arabidopsis thaliana. *Genet Mol Biol*. 41: 624–637.
Liu, S., Yu, F., Yang, Z., Wang, T., Xiong, H., Chang, C., et al. (2018) Establishment of dimethyl labeling-based quantitative acetylproteomics in Arabidopsis. *Mol Cell Proteomics*. 17: 1010–1027.
Luo, J., Tang, S., Peng, X., Yan, X., Zeng, X., Li, J., et al. (2015) Elucidation of cross-talk and specificity of early response mechanisms to salt and PEG-simulated drought stresses in brassica napus using comparative proteomic analysis. *PLoS One*. 10: 1–24.
Luo, Y., Wang, Z., Ji, H., Fang, H., Wang, S., Tian, L., et al. (2013) An Arabidopsis homolog of importin β1 is required for ABA response and drought tolerance. *Plant J*. 75: 377–389.
Madeira, F., Park, Y.M., Lee, J., Buso, N., Gur, T., Madhusoodanan, N., et al. (2019) The EMBL-EBI search and sequence analysis tools APIs in 2019. *Nucleic Acids Res*. 47: W636–W641.
Mei, Y., Gao, H.B., Yuan, M., and Xue, H.W. (2012) The Arabidopsis ARCP protein, CSI1, which is required for microtubule stability, is necessary for root and anther development. *Plant Cell*. 24: 1066–1080.
Mendel, R.R. (2002) Molybdoenzymes and molybdenum cofactor in plants. *J Exp Bot*. 53: 1689–1698.
Meng, M., Geisler, M., Johansson, H., Harholt, J., Scheller, H. V., Mellerowicz, E.J., et al. (2009) UDP-glucose pyrophosphorylase is not rate limiting, but is essential in arabidopsis. *Plant Cell Physiol*. 50: 998–1011.
Mergner, J., Frejno, M., List, M., Papacek, M., Chen, X., Chaudhary, A., et al. (2020) Mass-spectrometry-based draft of the Arabidopsis proteome. *Nature*. 579: 409–414.
Mittova, V., Tal, M., Volokita, M., and Guy, M. (2003) Up-regulation of the leaf mitochondrial and peroxisomal antioxidative systems in response to salt-induced oxidative stress in the wild salt-tolerant tomato species Lycopersicon pennellii. *Plant, Cell Environ*. 26: 845–856.
Mori, I.C., Murata, Y., Yang, Y., Munemasa, S., Wang, Y.F., Andreoli, S., et al. (2006) CDPKs CPK6 and CPK3 function in ABA regulation of guard cell S-type anion- and Ca2+- permeable channels and stomatal closure. *PLoS Biol*. 4: 1749–1762.

Mortimer, J.C., Laohavisit, A., Macpherson, N., Webb, A., Brownlee, C., Battey, N.H., et al. (2008) Annexins: Multifunctional components of growth and adaptation. *J Exp Bot*. 59: 533–544.

Moruno Algara, M., Kuczyńska-Wiśnik, D., Dębski, J., Stojowska-Swędrzyńska, K., Sominka, H., Bukrejewska, M., et al. (2019) Trehalose protects Escherichia coli against carbon stress manifested by protein acetylation and aggregation. *Mol Microbiol*. 112: 866–880.

Nallamilli, B.R.R., Edelmann, M.J., Zhong, X., Tan, F., Mujahid, H., Zhang, J., et al. (2014) Global analysis of lysine acetylation suggests the involvement of protein acetylation in diverse biological processes in rice (Oryza sativa). *PLoS One*. 9: 1–12.

O'Hara, L.E., Paul, M.J., and Wingler, A. (2013) How do sugars regulate plant growth and development? new insight into the role of trehalose-6-phosphate. *Mol Plant*. 6: 261–274.

Obendorf, R.L., and Gorecki, R.J. (2012) Soluble carbohydrates in legume seeds. *Seed Sci Res*. 22: 219–242.

Paez-Garcia, A., Motes, C.M., Scheible, W.R., Chen, R., Blancaflor, E.B., and Monteros, M.J. (2015) Root traits and phenotyping strategies for plant improvement. *Plants*. 4: 334–355.

Petricka, J.J., Schauer, M.A., Megraw, M., Breakfield, N.W., Thompson, J.W., Georgiev, S., et al. (2012) The protein expression landscape of the Arabidopsis root. *Proc Natl Acad Sci U S A*. 109: 6811–6818.

Pluskota, W.E., Szablińska, J., Obendorf, R.L., Górecki, R.J., and Lahuta, L.B. (2015) Osmotic stress induces genes, enzymes and accumulation of galactinol, raffinose and stachyose in seedlings of pea (Pisum sativum L.). *Acta Physiol Plant*. 37.

Quintero, F.J., Martinez-Atienza, J., Villalta, I., Jiang, X., Kim, W.Y., Ali, Z., et al. (2011) Activation of the plasma membrane Na/H antiporter salt-overly-sensitive 1 (SOS1) by phosphorylation of an auto-inhibitory C-terminal domain. *Proc Natl Acad Sci U S A*. 108: 2611–2616.

Rao, R.S.P., Thelen, J.J., and Miernyk, J.A. (2014) Is Lys-Ne{open}-acetylation the next big thing in post-translational modifications? *Trends Plant Sci*. 19: 550–553.

Reiland, S., Messerli, G., Baerenfaller, K., Gerrits, B., Endler, A., Grossmann, J., et al. (2009) Large-scale arabidopsis phosphoproteome profiling reveals novel chloroplast kinase substrates and phosphorylation networks1[w]. *Plant Physiol*. 150: 889–903.

Rest, J.S., Wilkins, O., Yuan, W., Purugganan, M.D., and Gurevitch, J. (2016) Meta-analysis and meta-regression of transcriptomic responses to water stress in Arabidopsis. *Plant J*. 85: 548–560.

Riboni, M., Test, A.R., Galbiati, M., Tonelli, C., and Conti, L. (2016) ABA-dependent control of GIGANTEA signalling enables drought escape via up-regulation of FLOWERING LOCUS T in Arabidopsis thaliana. *J Exp Bot*. 67: 6309–6322

Rutter, J., Probst, B.L., and McKnight, S.L. (2002) Coordinate regulation of sugar flux and translation by PAS kinase. *Cell*. 111: 17–28.

Saito, K. (2006) Sulfur Assimilatory Metabolism. The Long and Smelling Road. 136: 2443–2450.

Sakai, T., Honing, H. Van Der, Nishioka, M., Uehara, Y., Takahashi, M., Fujisawa, N., et al. (2008) Armadillo repeat-containing kinesins and a NIMA-related kinase are required for epidermal-cell morphogenesis in Arabidopsis. *Plant J*. 53: 157–171.

Sapiro, R., Tarantino, L.M., Velazquez, F., Kiriakidou, M., Hecht, N.B., Bucan, M., et al. (2000) Sperm antigen 6 is the murine homologue of the Chlamydomonas reinhardtii central apparatus protein encoded by the PF16 locus. *Biol Reprod*. 62: 511–518.

Schluepmann, H., and Matthew, P. (2009) Trehalose Metabolites in Arabidopsis — elusive , active and central Published By : The American Society of Plant Biologists Trehalose Metabolites in Arabidopsis — elusive , active and central. 7.

Schwalm, C.R., Anderegg, W.R.L., Michalak, A.M., Fisher, J.B., Biondi, F., Koch, G., et al. (2017) Global patterns of drought recovery. *Nature*. 548: 202–205.

Schwarz, G., and Mendel, R.R. (2006) Molybdenum Cofactor Biosynthesis and Molybdenum Enzymes. *Annu Rev Plant Biol*. 57: 623–647.

Seaton, D.D., Graf, A., Baerenfaller, K., Stitt, M., Millar, A.J., and Gruissem, W. (2018) Photoperiodic control of the Arabidopsis proteome reveals a translational coincidence mechanism . *Mol Syst Biol*. 14: 1–19.

Sharma, K., D'Souza, R.C.J., Tyanova, S., Schaab, C., Wiśniewski, J.R., Cox, J., et al. (2014) Ultradeep Human Phosphoproteome Reveals a Distinct Regulatory Nature of Tyr and Ser/Thr-Based Signaling. *Cell Rep*. 8: 1583–1594.

Shavrukov, Y., Kurishbayev, A., Jatayev, S., Shvidchenko, V., Zotova, L., Koekemoer, F., et al. (2017) Early flowering as a drought escape mechanism in plants: How can it aid wheat production? *Front Plant Sci*. 8: 1–8.

Shelden, M.C., Dias, D.A., Jayasinghe, N.S., Bacic, A., and Roessner, U. (2016) Root spatial metabolite profiling of two genotypes of barley (Hordeum vulgare L.) reveals differences in response to short-term salt stress. *J Exp Bot*. 67: 3731–3745.

Shi, H., Ishitani, M., Kim, C., and Zhu, J.K. (2000) The Arabidopsis thaliana salt tolerance gene SOS1 encodes a putative Na+/H+ antiporter. *Proc Natl Acad Sci U S A*. 97: 6896–6901.

Singh, P.K., Gao, W., Liao, P., Li, Y., Xu, F.C., Ma, X.N., et al. (2020) Comparative acetylome analysis of wild-type and fuzzless-lintless mutant ovules of upland cotton (Gossypium hirsutum Cv. Xu142) unveils differential protein acetylation may regulate fiber development. *Plant Physiol Biochem*. 150: 56–70.

Sirichandra, C., Davanture, M., Turk, B.E., Zivy, M., Valot, B., Leung, J., et al. (2010) The arabidopsis ABA-activated kinase OST1 phosphorylates the bZIP transcription factor ABF3 and creates a 14-3-3 binding site involved in its turnover. *PLoS One*. 5: 1–13.

Smith-Hammond, C.L., Swatek, K.N., Johnston, M.L., Thelen, J.J., and Miernyk, J.A. (2014) Initial description of the developing soybean seed protein Lys-Nε-acetylome. *J Proteomics*. 96: 56–66.

Sofroni, K., Takatsuka, H., Yang, C., Dissmeyer, N., Komaki, S., Hamamura, Y., et al. (2020) CDKD-dependent activation of CDKA;1 controls microtubule dynamics and cytokinesis during meiosis. *J Cell Biol*. 219.

Soufi, B., Soares, N.C., Ravikumar, V., and Macek, B. (2012) Proteomics reveals evidence of cross-talk between protein modifications in bacteria: Focus on acetylation and phosphorylation. *Curr Opin Microbiol*. 15: 357–363.

Szklarczyk, D., Morris, J.H., Cook, H., Kuhn, M., Wyder, S., Simonovic, M., et al. (2017) The STRING database in 2017: Quality-controlled protein-protein association networks, made broadly accessible. *Nucleic Acids Res*. 45: D362–D368.

Takahashi, H., Kopriva, S., Giordano, M., Saito, K., and Hell, R. (2011) Sulfur Assimilation in Photosynthetic Organisms: Molecular Functions and Regulations of Transporters and Assimilatory Enzymes. *Annu Rev Plant Biol*. 62: 157–184.

Takatsuka, H., Ohno, R., and Umeda, M. (2009) The Arabidopsis cyclin-dependent kinase-activating kinase CDKF;1 is a major regulator of cell proliferation and cell expansion but is dispensable for CDKA activation. *Plant J*. 59: 475–487.

Tran, H.T., Nimick, M., Uhrig, R.G., Templeton, G., Morrice, N., Gourlay, R., et al. (2012) Arabidopsis thaliana histone deacetylase 14 (HDA14) is an α-tubulin deacetylase that associates with PP2A and enriches in the microtubule fraction with the putative histone acetyltransferase ELP3. *Plant J*. 71: 263–272.

Tyanova, S., Temu, T., Sinitcyn, P., Carlson, A., Hein, M.Y., Geiger, T., et al. (2016) The Perseus computational platform for comprehensive analysis of (prote)omics data. *Nat Methods*. 13: 731–740.

Uga, Y., Sugimoto, K., Ogawa, S., Rane, J., Ishitani, M., Hara, N., et al. (2013) Control of root system architecture by DEEPER ROOTING 1 increases rice yield under drought conditions. *Nat Genet*. 45: 1097–1102.

Uhrig, R.G., Schläpfer, P., Roschitzki, B., Hirsch-Hoffmann, M., and Gruissem, W. (2019) Diurnal changes in concerted plant protein phosphorylation and acetylation in Arabidopsis organs and seedlings. *Plant J*. 99: 176–194.

Ullah, A., Dutta, D., and Fliegel, L. (2016) Expression and characterization of the SOS1 Arabidopsis salt tolerance protein. *Mol Cell Biochem*. 415: 133–143.

Uno, Y., Furihata, T., Abe, H., Yoshida, R., Shinozaki, K., and Yamaguchi-Shinozaki, K. (2000) Arabidopsis basic leucine zipper transcription factors involved in an abscisic acid-dependent signal transduction pathway under drought and high-salinity conditions. *Proc Natl Acad Sci U S A*. 97: 11632–11637.

Verslues, P.E., and Juenger, T.E. (2011) Drought, metabolites, and Arabidopsis natural variation: A promising combination for understanding adaptation to water-limited environments. *Curr Opin Plant Biol*. 14: 240–245.

Walley, J.W., Shen, Z., McReynolds, M.R., Schmelz, E.A., and Briggs, S.P. (2018) Fungal-induced protein hyperacetylation in maize identified by acetylome profiling. *Proc Natl Acad Sci U S A*. 115: 210–215.

Wasson, A.P., Richards, R.A., Chatrath, R., Misra, S.C., Prasad, S.V.S., Rebetzke, G.J., et al. (2012) Traits and selection strategies to improve root systems and water uptake in water-limited wheat crops. *J Exp Bot*. 63: 3485–3498.

Weinert, B.T., Wagner, S.A., Horn, H., Henriksen, P., Liu, W.R., Olsen, J. V., et al. (2011) Proteome-wide mapping of the Drosophila acetylome demonstrates a high degree of conservation of lysine acetylation. *Sci Signal*. 4: 1–12.

Willems, P., Horne, A., Van Parys, T., Goormachtig, S., De Smet, I., Botzki, A., et al. (2019) The Plant PTM Viewer, a central resource for exploring plant protein modifications. *Plant J*. 99: 752–762.

Wu, F., Chi, Y., Jiang, Z., Xu, Y., Xie, L., Huang, F., et al. (2020) Hydrogen peroxide sensor HPCA1 is an LRR receptor kinase in Arabidopsis. *Nature*. 578: 577–581.

Wu, X., Gong, F., Cao, D., Hu, X., and Wang, W. (2016) Advances in crop proteomics: PTMs of proteins under abiotic stress. *Proteomics*. 16: 847–865.

Wu, X., Oh, M.H., Schwarz, E.M., Larue, C.T., Sivaguru, M., Imai, B.S., et al. (2011) Lysine acetylation is a widespread protein modification for diverse proteins in Arabidopsis. *Plant Physiol*. 155: 1769–1778.

Xiong, L., Ishitani, M., Lee, H., and Zhu, J.K. (2001) The Arabidopsis LOS5/ABA3 locus encodes a molybdenum cofactor sulfurase and modulates cold stress- and osmotic stress-responsive gene expression. *Plant Cell*. 13: 2063–2083.

Xu, P., Cai, X.T., Wang, Y., Xing, L., Chen, Q., and Xiang, C. Bin (2014) HDG11 upregulates cell-wall-loosening protein genes to promote root elongation in Arabidopsis. *J Exp Bot*. 65: 4285–4295.

Xu, P., Zang, A., Chen, H., and Cai, W. (2016) The small G protein AtRAN1 regulates vegetative growth and stress tolerance in arabidopsis thaliana. *PLoS One*. 11: 1–15.

Xue, C., Liu, S., Chen, C., Zhu, J., Yang, X., Zhou, Y., et al. (2018) Global Proteome Analysis Links Lysine Acetylation to Diverse Functions in Oryza Sativa. *Proteomics*. 18.

Yan, C., Yan, Z., Wang, Y., Yan, X., and Han, Y. (2014) Tudor-SN, a component of stress granules, regulates growth under salt stress by modulating GA20ox3 mRNA levels in Arabidopsis. *J Exp Bot*. 65: 5933–5944.

Yang, W.Y., Zheng, Y., Bahn, S.C., Pan, X.Q., Li, M.Y., Vu, H.S., et al. (2012) The patatin-containing phospholipase A pPLAIIα modulates oxylipin formation and water loss in arabidopsis thaliana. *Mol Plant*. 5: 452–460.

Yi, D.G., and Huh, W.K. (2015) UDP-glucose pyrophosphorylase Ugp1 is involved in oxidative stress response and long-term survival during stationary phase in Saccharomyces cerevisiae. *Biochem Biophys Res Commun*. 467: 657–663.

Yin, H., Li, M., Li, D., Khan, S.A., Hepworth, S.R., and Wang, S.M. (2019) Transcriptome analysis reveals regulatory framework for salt and osmotic tolerance in a succulent xerophyte. *BMC Plant Biol*. 19: 1–15.

Yoshida, T., Fujita, Y., Maruyama, K., Mogami, J., Todaka, D., Shinozaki, K., et al. (2015) Four Arabidopsis AREB/ABF transcription factors function predominantly in gene expression downstream of SnRK2 kinases in abscisic acid signalling in response to osmotic stress. *Plant, Cell Environ*. 38: 35–49.

Zhang, H., Han, B., Wang, T., Chen, S., Li, H., Zhang, Y., et al. (2012) Mechanisms of plant salt response: Insights from proteomics. *J Proteome Res*. 11: 49–67.

Zhang, H., Liu, D., Yang, B., Liu, W.Z., Mu, B., Song, H., et al. (2020) Arabidopsis CPK6 positively regulates ABA signaling and drought tolerance through phosphorylating ABA-responsive element-binding factors. *J Exp Bot*. 71: 188–203.

Zhao, S., Xu, W., Jiang, W., Yu, W., Lin, Y., Zhang, T., et al. (2010) Regulation of Cellular Metabolism by Protein Lysine Acetylation. *Science (80-)*. 1000–1004.

Zhou, H., Finkemeier, I., Guan, W., Tossounian, M.A., Wei, B., Young, D., et al. (2018) Oxidative stress-triggered interactions between the succinyl- and acetyl-proteomes of rice leaves. *Plant Cell Environ*. 41: 1139–1153.

Zhu, J.K. (2016) Abiotic Stress Signaling and Responses in Plants. *Cell*. 167: 313–324.

TABLES

Table 1: Summary results of proteomic and PTMomics analyses of Arabidopsis roots after 24 h of salt and osmotic stress (n=3). The last two columns depict the number (%) of significantly changing PTMs occurring on proteins either [ii]exhibiting or [i]not exhibiting a corresponding change in protein abundance is shown.

Stress	Proteome Assessed	*Quantified		**Significantly Changing under Stress		[i]Number (%) of Sig PTM Quantified not Exhibiting Proteome Changes	[ii]Number (%) of Sig PTM Quantified Exhibiting Proteome Changes
		Proteins	Peptides	Proteins	Peptides	Proteins	Proteins
300mM Mannitol (Osmotic)	Acetylproteome (Ac)	201	266	24	25	17 (71%)	0 (0%)
	Phosphoproteome (P)	1291	3681	142	175	31 (21.9%)	0 (0%)
	Proteome (TP)	3128	n/a	32	*n/a*	*n/a*	*n/a*
150mM NaCl (Salinity)	Acetylproteome (Ac)	201	266	22	25	13 (59%)	0 (0%)
	Phosphoproteome (P)	1291	3681	160	203	39 (24.4%)	0 (0%)
	Proteome (TP)	3128	*n/a*	86	*n/a*	*n/a*	*n/a*

*Quantified PTM (Ac & P) = Localization ≥ 0.75

*Quantified Proteome (TP) = min 2 peptides per protein

**Significantly changing under stress (Ac, P & TP) = *p-val* ≤ 0.05 and ≥ 1.5 fold-change in PTM abundance

Table 2: Enriched GO terms for significant protein abundance changes upon 24 h of 150 mM salt (NaCl) treatment

GO Term	GO ID	pvalue	BH pvalue
organonitrogen compound metabolic process	GO:1901564	3.63E-06	6.51E-04
S-glycoside metabolic process	GO:0016143	7.48E-06	0.001207625546
translational elongation	GO:0006414	2.01E-05	0.002457265017
glycosyl compound biosynthetic process	GO:1901659	2.20E-05	0.00257978525
sulfate reduction	GO:0019419	1.42E-04	0.01381235311
glycosinolate metabolic process	GO:0019757	1.44E-04	0.01381235311
glycosinolate biosynthetic process	GO:0019758	1.96E-04	0.01814212421
translation	GO:0006412	2.10E-04	0.01882462124
regulation of endopeptidase activity	GO:0052548	4.64E-04	0.03122389969
response to osmotic stress	GO:0006970	4.81E-04	0.03157020814
organonitrogen compound biosynthetic process	GO:1901566	6.49E-04	0.03968781631
protein dephosphorylation	GO:0006470	7.03E-04	0.04111057319

glycosyl compound metabolic process	GO:1901657	8.62E-04	0.04916442018
cellular amino acid metabolic process	GO:0006520	8.77E-04	0.04916442018
Protein Domain Name	**AGI**	**Domain**	**BH pvalue**
Chaperonin Cpn60/TCP-1 family	AT1G24510,AT3G02530,AT3G03960,AT3G11830,AT5G20890,AT5G26360,AT5G56500	IPR002423	0.0001977420788
Heat shock protein 70 family	AT3G09440,AT4G37910,AT5G02500,AT5G09590,AT5G28540,AT5G42020	IPR013126	0.001032156851
Pyridoxal phosphate-dependent transferase	AT1G23310,AT1G43710,AT1G80600,AT2G13360,AT2G20610,AT3G01120,AT4G32520,AT4G35630,AT5G17330,AT5G26780,AT5G46180	IPR015424	0.001649480794
Thioredoxin-like superfamily	AT1G02920,AT1G09640,AT1G35620,AT1G45145,AT1G49860,AT1G57720,AT1G62180,AT1G65980,AT1G75270,AT2G47470,AT3G09270,AT4G02520,AT4G04610,AT4G04950,AT4G21990,AT4G27080,AT5G08290,AT5G47890	IPR036249	0.002955649486
Glutathione S-transferase, C-terminal	AT1G02920,AT1G09640,AT1G49860,AT1G57720,AT3G09270,AT4G02520	IPR004046	0.003395888372
NAD(P)-binding domain superfamily	AT1G04410,AT1G08200,AT1G13440,AT1G15950,AT1G31230,AT1G53240,AT1G63000,AT1G64190,AT1G67730,AT1G79530,AT3G07690,AT3G15290,AT3G19450,AT3G25530,AT3G58610,AT3G61220,AT4G34230,AT5G08300,AT5G14780,AT5G28840,AT5G43330	IPR036291	0.003434118093
Hyaluronan/mRNA-binding protein	AT4G16830,AT4G17520,AT5G47210	IPR006861	0.004099704067
Aminoacyl-tRNA synthetase, class I, conserved site	AT1G14610,AT1G25350,AT1G66530,AT4G10320,AT4G13780	IPR001412	0.004388306174
Six-bladed beta-propeller, TolB-like	AT1G21670,AT1G74020,AT2G01410,AT2G47390,AT3G57020,AT5G39970	IPR011042	0.01776705313
Glycoside hydrolase superfamily	AT1G47600,AT1G51470,AT3G13750,AT3G18080,AT3G52840,AT3G60130,AT4G19810,AT5G07830,AT5G08380,AT5G26000,AT5G40390,AT5G49360,AT5G56870,AT5G63800	IPR017853	0.02231435074
Histidine kinase/HSP90-like ATPase	AT2G04030,AT3G07770,AT4G24190,AT5G56010,AT5G56030	IPR003594	0.03531610162
6-phosphogluconate dehydrogenase-like, C-terminal domain superfamily	AT1G64190,AT3G07690,AT3G15290,AT3G25530,AT3G58610	IPR008927	0.03531610162

928

FIGURES

Figure 1:

Proteome and PTMome changes under osmotic or salt stress. (A) Experimental workflow (B-D) Venn diagram and Log_2 fold-change (FC) scatterplots for significantly changing (B) acetylome, (C) phosphoproteome and (D) proteome (unmodified proteins) across biological replicates (n=3). PTM-levels are plotted based on the median Log_2FC of all modified peptides for each protein. (E) Subcellular localization distribution of significantly changing proteins in abundance or PTM-level (*pval* ≤ 0.05; FC ≥ 1.5).

Figure 2:

Comparison of transcript-level changes with corresponding protein abundance, phosphorylation, and lysine acetylation changes upon 24 h of osmotic stress. Transcript-level changes corresponding to significantly changing proteins (either abundance or for each PTM) in our study were calculated from previously described microarray experiments (KIllan et al., 2007) and clustered by longitudinal shape.

Figure 3:

Comparison of transcript-level changes with corresponding protein abundance, phosphorylation, and lysine acetylation changes upon 24 h of salt stress. Transcript-level changes corresponding to significantly changing proteins in our study (either based on abundance or for each PTM) were calculated from previously described microarray experiments (Killan et al., 2007) and clustered by longitudinal shape.

Figure 4:

Association network of Arabidopsis root under 24 h 150 mM salt (NaCl). STRING database association network shown for proteins significantly changing in their total protein, phosphorylation, or lysine acetylation status. The maximal log_2FC change ranges from -2.5 (Max log_2FC EN) to +2.5 (Max log_2FC ED). Edge thickness equates to confidence in association. Inner circle represents subcellular localization (SUBA 4; https://suba.live/): cytosol (red), mitochondria (purple), nucleus (blue), peroxisome (green), plasma membrane (beige), plastid (amber), vacuole (lavender), endoplasmic reticulum/extracellular/Golgi (grey). Outer ring represents protein status: total protein change (1st division), phosphorylation (2nd division), lysine acetylation (3rd division). Grey clusters depict proteins belonging to a common cellular process. Proteins with an edge score threshold of 0.5 or below were excluded from visualization.

Figure 5:

Association network of Arabidopsis root under 24 h 300 mM mannitol. STRING database association network shown for proteins significantly changing in their total protein, phosphorylation, or lysine acetylation status. The maximal log_2FC change ranges from -2.5 (Max log_2FC EN) to +2.5 (Max log_2FC ED). Edge thickness equates to confidence in association. Inner circle represents subcellular localization (SUBA 4; https://suba.live/): cytosol (red), mitochondria (purple), nucleus (blue), peroxisome (green), plasma membrane (beige), plastid (amber), vacuole (lavender), endoplasmic reticulum/extracellular/Golgi (grey). Outer ring represents protein status: total protein change (1st division), phosphorylation (2nd division), lysine acetylation (3rd division). Grey clusters depict proteins belonging to a common cellular process. Proteins with an edge score threshold of 0.5 or below were excluded from visualization.

.

SUPPLEMENTAL INFORMATION

Supplemental Table 1: Results of the proteome analysis

Supplemental Table 2: Results of the phosphoproteome analysis

Supplemental Table 3: Results of acetylome analysis

Supplemental Table 4: Gene Ontology and protein domain enrichment for proteins with significantly changing abundance upon osmotic and salt stress.

Supplemental Table 5: Transcript data clustering analysis

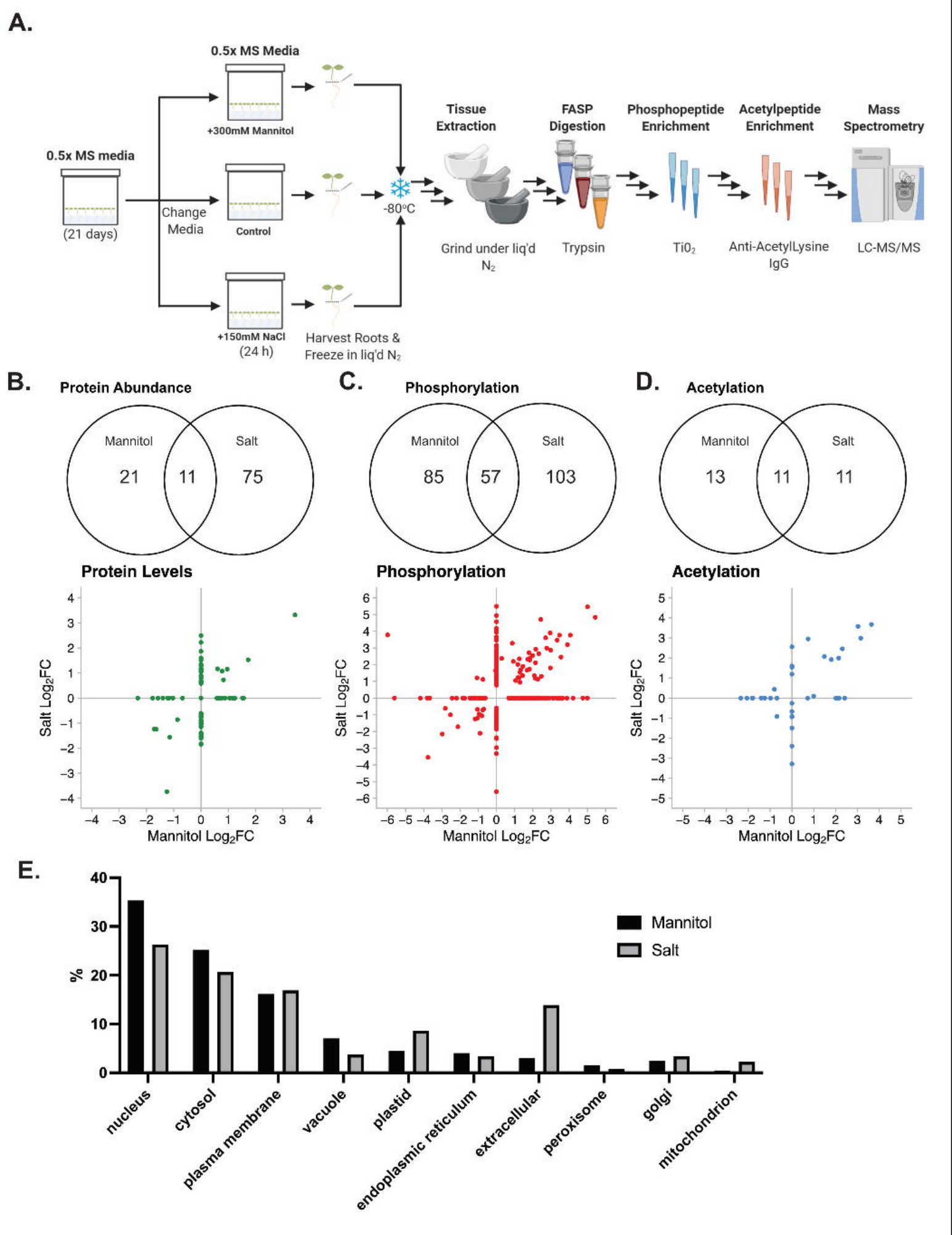
A.
0.5x MS Media
+300mM Mannitol
0.5x MS media
(21 days)
Change Media
Control
+150mM NaCl
(24 h)
Harvest Roots & Freeze in liq'd N2
-80°C
Tissue Extraction
Grind under liq'd N2
FASP Digestion
Trypsin
Phosphopeptide Enrichment
Ti02
Acetylpeptide Enrichment
Anti-AcetylLysine IgG
Mass Spectrometry
LC-MS/MS
B.
Protein Abundance
Mannitol
Salt
21
11
75
C.
Phosphorylation
Mannitol
Salt
85
57
103
D.
Acetylation
Mannitol
Salt
13
11
11
Protein Levels
Phosphorylation
Acetylation
Salt Log2FC
Mannitol Log2FC
E.
%
Mannitol
Salt
nucleus
cytosol
plasma membrane
vacuole
plastid
endoplasmic reticulum
extracellular
peroxisome
golgi
mitochondrion

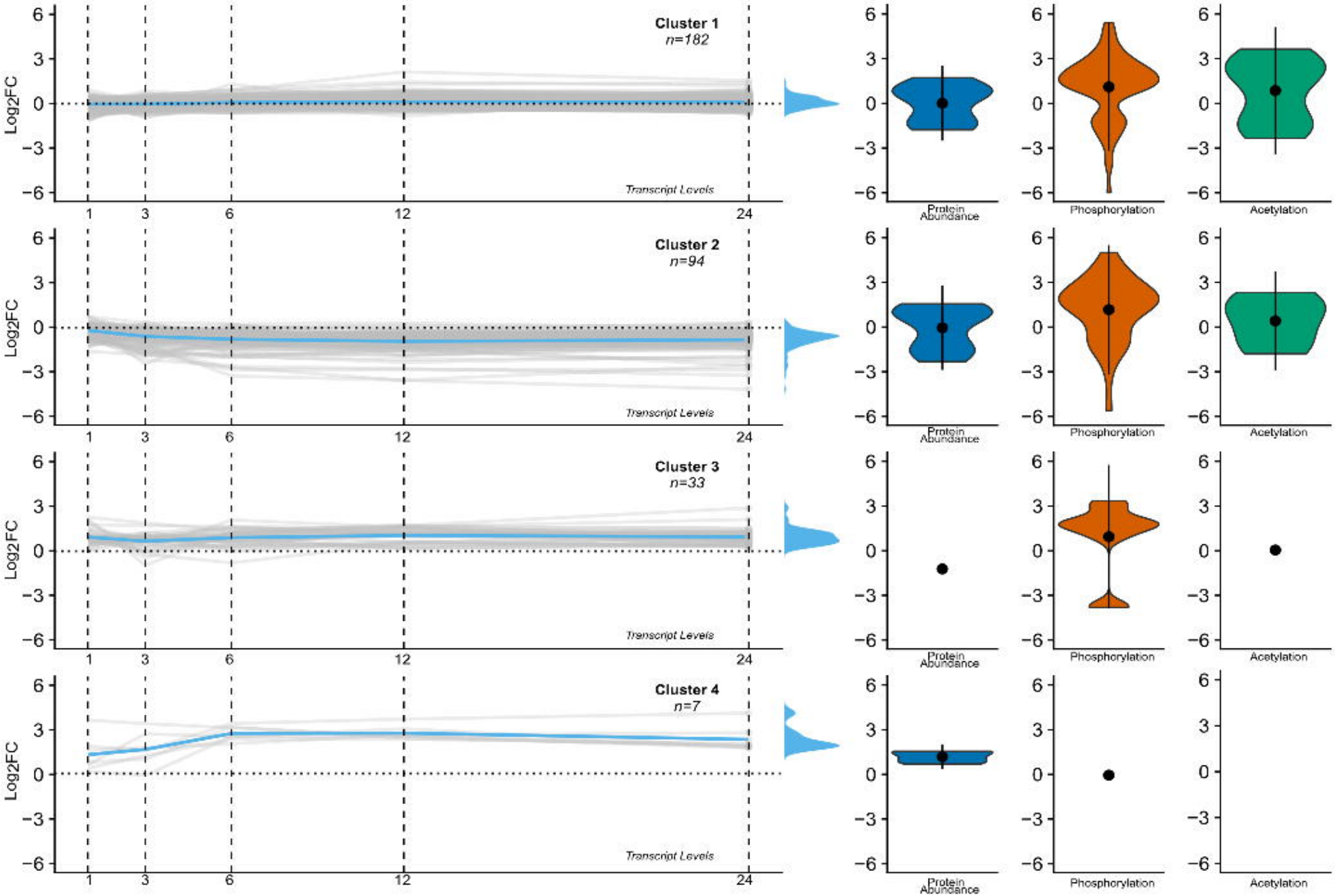
Cluster 1
n=182
Cluster 2
n=94
Cluster 3
n=33
Cluster 4
n=7
Log2FC
Transcript Levels
1
3
6
12
24
Protein Abundance
Phosphorylation
Acetylation

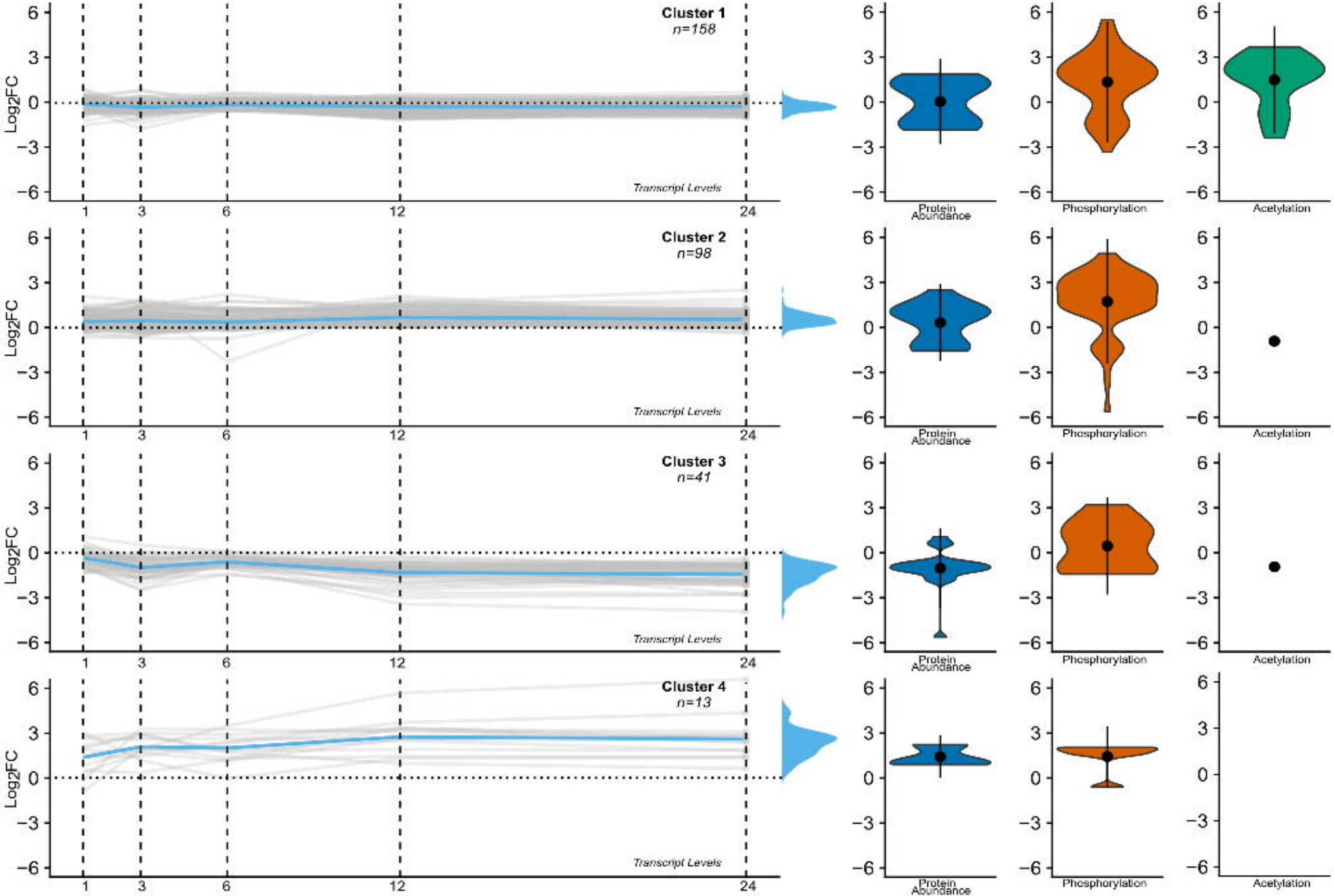
Cluster 1
n=158
Cluster 2
n=98
Cluster 3
n=41
Cluster 4
n=13
Log2FC
6
3
0
−3
−6
Transcript Levels
1
3
6
12
24
Protein Abundance
Phosphorylation
Acetylation

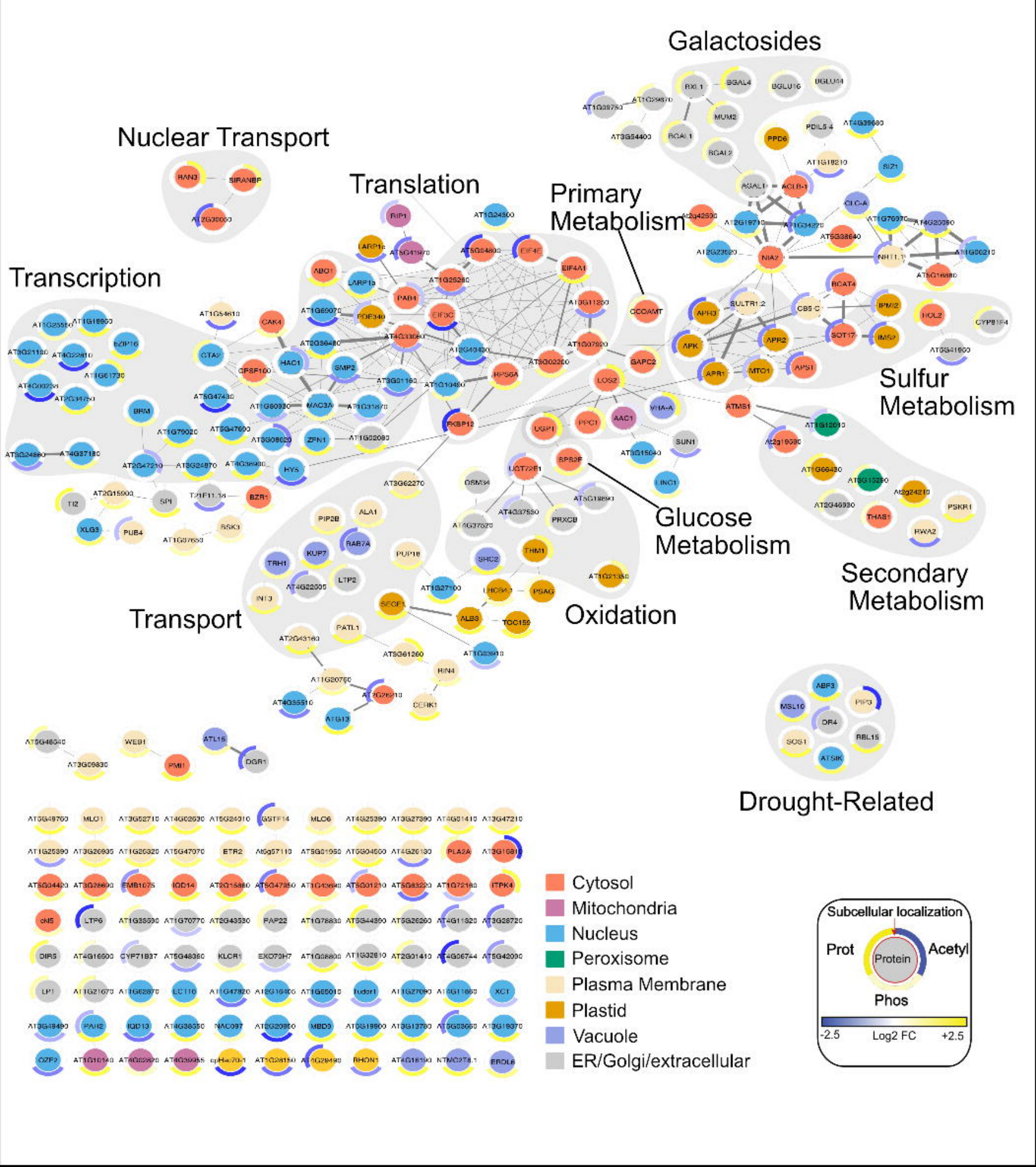
Galactosides
Nuclear Transport
Translation
Primary Metabolism
Transcription
Sulfur Metabolism
Glucose Metabolism
Secondary Metabolism
Transport
Oxidation
Drought-Related
Cytosol
Mitochondria
Nucleus
Peroxisome
Plasma Membrane
Plastid
Vacuole
ER/Golgi/extracellular
Subcellular localization
Prot
Acetyl
Protein
Phos
-2.5
Log2 FC
+2.5

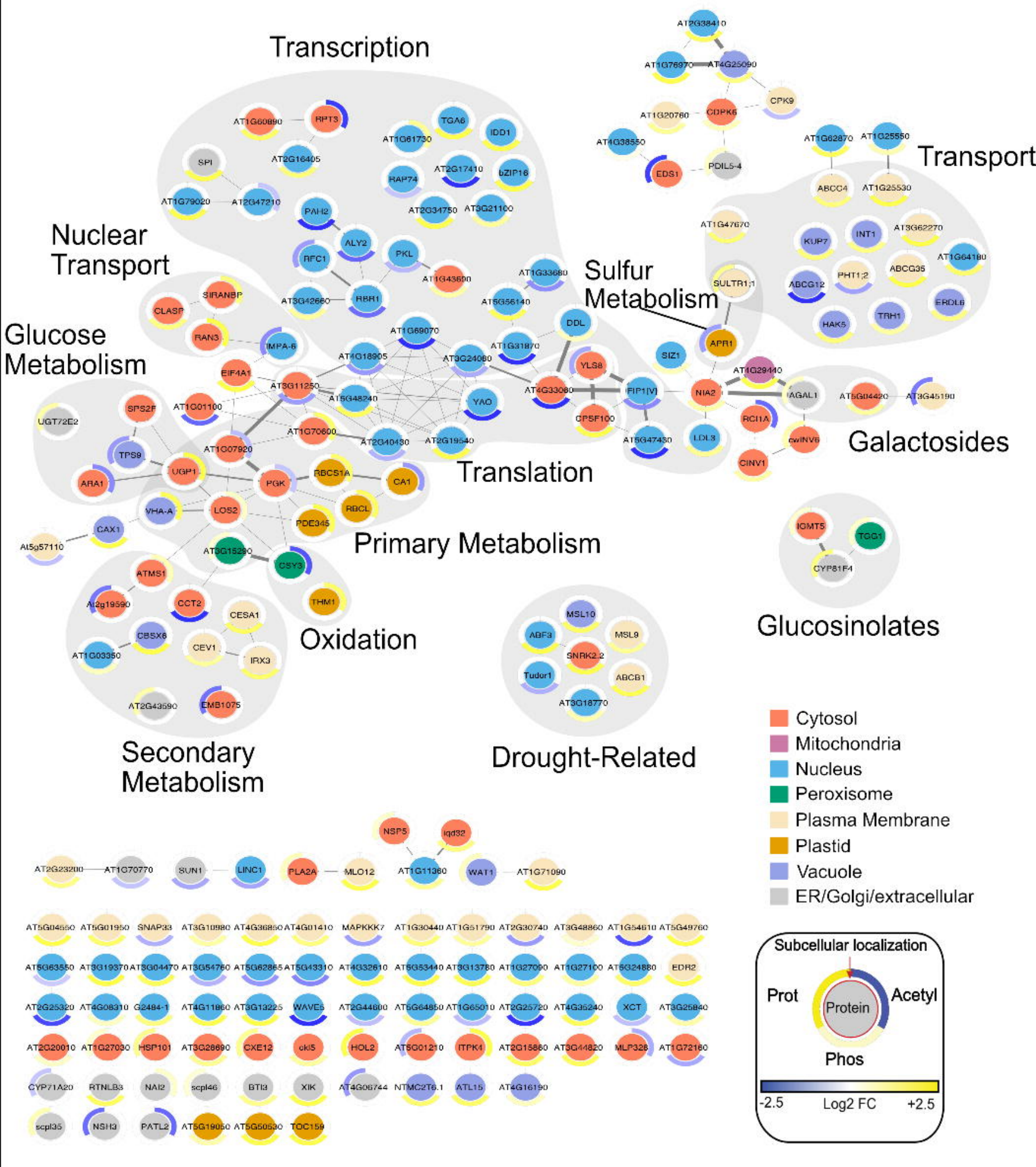
Transcription
Transport
Nuclear Transport
Sulfur Metabolism
Glucose Metabolism
Translation
Galactosides
Primary Metabolism
Glucosinolates
Oxidation
Secondary Metabolism
Drought-Related
AT2G38410
AT1G76970
AT4G25090
CPK9
AT1G20760
CDPK6
AT4G38550
EDS1
PDIL5-4
AT1G62870
AT1G25550
ABCC4
AT1G25530
AT1G47670
KUP7
INT1
AT3G62270
AT1G64180
PHT1;2
ABCG35
ABCG12
ERDL6
HAK5
TRH1
SULTR1;1
APR1
SIZ1
AT1G29440
NIA2
AGAL1
AT5G04420
AT3G45190
RCI1A
cwINV6
CINV1
LDL3
AT5G47430
CPSF100
FIP1[V]
AT4G33080
YLS8
DDL
AT1G33680
AT5G56140
AT1G31870
AT3G24080
AT1G69070
AT4G18905
YAO
AT2G19540
AT2G40430
AT1G70600
AT3G11250
AT5G48240
AT1G01100
AT1G07920
EIF4A1
IMPA-6
RAN3
CLASP
SIRANBP
AT3G42660
RBR1
PKL
AT1G43600
RFC1
ALY2
PAH2
AT2G34750
AT3G21100
AT2G17410
bZIP16
RAP74
AT1G61730
TGA6
IDD1
AT1G60890
RPT3
AT2G16405
SPI
AT1G79020
AT2G47210
SPS2F
UGT72E2
TPS9
ARA1
UGP1
PGK
RBCS1A
CA1
RBCL
PDE345
VHA-A
LOS2
CAX1
At5g57110
AT3G15290
CSY3
ATMS1
At2g19590
CCT2
CESA1
CBSX6
AT1G03350
CEV1
IRX3
THM1
AT2G43590
EMB1075
IGMT5
TGG1
CYP81F4
MSL10
ABF3
MSL9
SNRK2.2
Tudor1
ABCB1
AT3G18770
Cytosol
Mitochondria
Nucleus
Peroxisome
Plasma Membrane
Plastid
Vacuole
ER/Golgi/extracellular
NSP5
Iqd32
AT2G23200
AT1G70770
SUN1
LINC1
PLA2A
MLO12
AT1G11360
WAT1
AT1G71090
AT5G04550 AT5G01950 SNAP33 AT3G10980 AT4G36850 AT4G01410 MAPKKK7 AT1G30440 AT1G51790 AT2G30740 AT3G48860 AT1G54610 AT5G49760
AT5G63550 AT3G19370 AT3G04470 AT3G54750 AT5G62865 AT5G43310 AT4G32610 AT5G53440 AT3G13780 AT1G27090 AT1G27100 AT5G24880 EDR2
AT2G25320 AT4G08310 G2484-1 AT4G11860 AT3G13225 WAVE5 AT2G44600 AT5G64850 AT1G65010 AT2G25720 AT4G35240 XCT AT3G25840
AT2G20010 AT1G27030 HSP101 AT3G28690 CXE12 ckl5 HOL2 AT5G01210 ITPK1 AT2G15860 AT3G44820 MLP328 AT1G72160
CYP71A20 RTNLB3 NAI2 scpl46 BTI3 XIK AT4G06744 NTMC2T6.1 ATL15 AT4G16190
scpl35 NSH3 PATL2 AT5G19050 AT5G50530 TOC159
Subcellular localization
Prot
Acetyl
Protein
Phos
-2.5
Log2 FC
+2.5